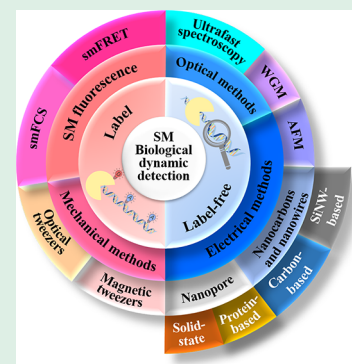


Single-Molecule Nanotechnologies: An Evolution in Biological Dynamics Detection

Yu Li,[†] Lihua Zhao,[†] Yuan Yao, and Xuefeng Guo*[‡]

Beijing National Laboratory for Molecular Sciences, State Key Laboratory for Structural Chemistry of Unstable and Stable Species, College of Chemistry and Molecular Engineering, Peking University, Beijing 100871, P. R. China

ABSTRACT: Single-molecule detection is a rapidly developing area within the analytical chemistry field that requires ultrasensitive technologies to detect a range of molecules. Over the past few decades, various optically-, mechanically-, and electrically-based strategies have been employed for single-molecule detection to uncover information in biological processes. These strategies enable real-time monitoring with single-molecule/single-event sensitivity. In addition, their high temporal resolution enables investigation of the underlying mechanisms of biological functions from static to dynamic, from qualitative to quantitative, and from one to multiple disciplines. In this review, we provide a brief overview of the prominent, real-time single-molecule detection nanotechnologies and their potential applications within the life science fields.



KEYWORDS: biological dynamics, single-molecule detection, label free, single-molecule sensitivity, real-time detection

1. INTRODUCTION

The scientific community has sought to reveal the biomolecular pathways that enable the diverse and complex functions of proteins, cells, and tissues. Significant efforts over the past few decades have revealed static, single-molecular structures of biomolecules using various techniques. For example, cryo-electron microscopy (cryo-EM) has become a powerful technique used to determine the conformational states of biomolecular structures with near atomic-level resolution. High-resolution X-ray crystallography has revolutionized the understanding of protein functions with atomic resolution. However, probing the dynamic activities of individual biomolecules enables a more accurate understanding of their behaviors and thus biological functions. This understanding facilitates the rapid development of precision medicine and other clinical applications.

Single-molecule detection pushes the limit of chemical analysis because, to obtain a signal from a single molecule, the technology must (1) be highly sensitive, to read weak signals from individual molecules and (2) have a superior signal-to-noise ratio to extract target signals over the background. With a surge in revolutionary nanotechnologies over the last few decades, various single-molecule techniques have been developed. Since the 1950s, when Richard Feynman stated that “there is plenty of room at the bottom”, scientists have been actively investigating areas of small length scales.¹ Today, single-molecule detection plays a significant role in fundamental investigations in different fields such as biochemistry, biophysics, biotechnology, immunology, DNA sequencing, and medical diagnosis.^{2–6} The wide-field microscope was developed in the late 1980s for single-molecule detection.^{7–9} Initially, individual chromophores embedded in a crystal matrix

were observed in a cryogenic substrate. Several years later, imaging single molecules under ambient conditions was reported, which enabled disclosure of the underlying information in the ensemble measurement, thus opening single-molecule tools to broad applications in the life science field.^{10,11}

Beyond understanding of the mean features of complex biomolecules mined from ensemble measurements, single-molecule detection can characterize the intrinsic properties and dynamic functions of individual molecules, aiding in overcoming desynchronization in ensemble-average experiments that blur kinetic analyses. Instead of smooth consecutive transitions caused by the flattening effect in asynchronous ensemble approaches, single-molecule measurements record and analyze dwell time and the distribution of individual molecules at certain states along a pathway, thus revealing both the underlying statistical properties of the dynamic process and the mean reaction kinetics.

A diverse range of single-molecule nanotechnologies has been employed to monitor molecular heterogeneity to establish structure–function relationships in dynamic biological systems. The primary approaches have been divided as labeled and label-free nanotechnologies in this review (Table 1). This review highlights the unique advantages and importance of several key approaches developed for probing single-molecule dynamic processes in biology. A brief,

Special Issue: Young Investigator Forum

Received: September 15, 2019

Accepted: December 25, 2019

Published: December 25, 2019

Table 1. Capabilities and Applications of Common Single-Molecule Detection Methods in Biological Dynamics Investigations^a

attributes	label single-molecule nanotechnologies			label-free single-molecule nanotechnologies					
	smFRET	smFCS	optical tweezer	magnetic tweezer	ultrafast spectroscopy	WGM	AEM	nanocarbons- and nanowires-based electronic device	nanopore
temporal resolution	0.1 ms	1 μ s	10 ms	30 ms	1 fs	1 ps	30 ms	0.1 μ s	1 μ s
label	fluorophores or dyes	fluorophores or dyes <i>in vivo</i> detection and imaging	dielectric beads	magnetic beads	none	none	none	none	none
features	spectroscopic ruler	three-dimensional manipulation	twisting force	high temporal resolution	high temporal resolution	high temporal resolution	three-dimensional imaging	long duration recording	low-cost DNA sequencing
typical applications	structural dynamics of proteins and protein complexes, ^{12–16} time scales of protein, DNA and RNA dynamics, ^{17–20} dynamics of biomolecular interactions ^{21,22}	dynamics of biomolecular reactions, ²³ diffusion coefficients, ²⁴ affinity constants ²⁵	transition-state analysis, ^{26,27} force–extension analysis, ^{28,29} force-manipulation assays ³⁰	transition-state analysis, ³¹ force-torsion analysis, ^{32,33} DNA topology, ^{33,34} interactions involving DNA or RNA ³⁵	light-harvesting processes of photosynthetic pigment–protein complexes ^{36–39}	dynamics of single-biomolecular binding events ^{40,41}	transition-state analysis, ⁴² force–extension analysis ⁴³	enzyme activity, ^{44–47} dynamics of biomolecular interactions, ⁴⁸ motion of molecular motors, ^{49,50} DNA hybridization, ^{51–53} time scales of DNA or RNA dynamics ^{47,54}	DNA sequencing, ^{55,56} interactions involving DNA ⁵⁷

^aSM, single molecule; FRET, Förster resonance energy transfer; FCS, fluorescence correlation spectroscopy; WGM, whispering gallery mode; AEM, atomic force microscopy.

historical overview will be presented, and key advances will be highlighted. This review also discusses the challenges that currently exist for single-molecule detection and briefly discusses how these shortcomings can be solved with the advancement of technology. Considering the limited space in this review, we did not include the high-resolution single-molecule imaging technique known as STORM, which is one of the most exciting technique advances in the past few decades.

2. LABELED SINGLE-MOLECULE NANOTECHNOLOGIES

In labeled single-molecule nanotechnologies, labels are used to relay photonic or mechanical information regarding the molecule's behavior to the detection system. Conventional labels are fluorophores/dyes for fluorescence techniques and dielectric/magnetic beads for optical or magnetic tweezers. In this section, we summarize the diverse range of labeled single-molecule nanotechnologies, divided by the label mechanism that is employed, and the advancements contributed by the nanotechnology.

2.1. Single-Molecule Fluorescence. Fluorescence was discovered in the 16th century⁵⁸ and was named in 1852 by George Gabriel Stokes.⁵⁹ Fluorescence occurs when a photosensitive fluorophore or dye molecule becomes electronically excited by absorbing energy from incident light. The excited electron relaxes to the electronic ground state and emits lower frequency light, known as fluorescent light, which can be detected through various methods, such as a fluorescent microscope.⁶⁰ However, fluorescence microscopy has a poor fluorescence resolution limit, making room for advanced techniques such as random excitation point molecular positioning superposition and spatial modulation structure light illumination.

Background fluorescence can be effectively reduced by selective emission (collecting emission from a small focusing volume) and selective excitation (illuminating a small part of the sample).⁶¹ Confocal microscopy and spinning disk confocal microscopy⁶² were developed on the basis of selective emission. Selective excitation is used in a variety of other microscopic techniques⁶³ including total internal reflection fluorescence (TIRF) microscopy,⁶⁴ selective plane illumination microscopy,⁶⁵ and two-photon excitation microscopy.⁶⁶ These microscopic techniques have a high signal-to-noise ratio and imaging quality, which enable single-molecule detection. After two significant technological breakthroughs, using liquid helium at room temperature⁶⁷ and detection in solution, a single myosin protein was studied by TIRF microscopy in 1995.¹¹ Subsequently, an explosion of studies that image complex biological functions, such as the motion of molecular motors,^{68,69} protein dynamics,^{70,71} nucleic acid dynamics,^{61,72} and biomolecular interactions,⁷³ were reported using single-molecule fluorescence microscopy.

2.1.1. Single-Molecule Förster Resonance Energy Transfer (smFRET). Förster resonance energy transfer (FRET) can be used as a “spectroscopic ruler” to identify the distance between two fluorophores or dyes in the range of 1–10 nm.⁵ This system was first discovered by Cario, Franck, and Perrin in 1923.⁷⁴ The energy stored in the excited electronic states of the excited fluorophore or dye (“donor”) is transferred to another fluorophore or dye (“acceptor”) by dipole–dipole interactions.⁷⁵ Consequently, the excited donor electrons relax to the ground state and excite the acceptor electrons to the

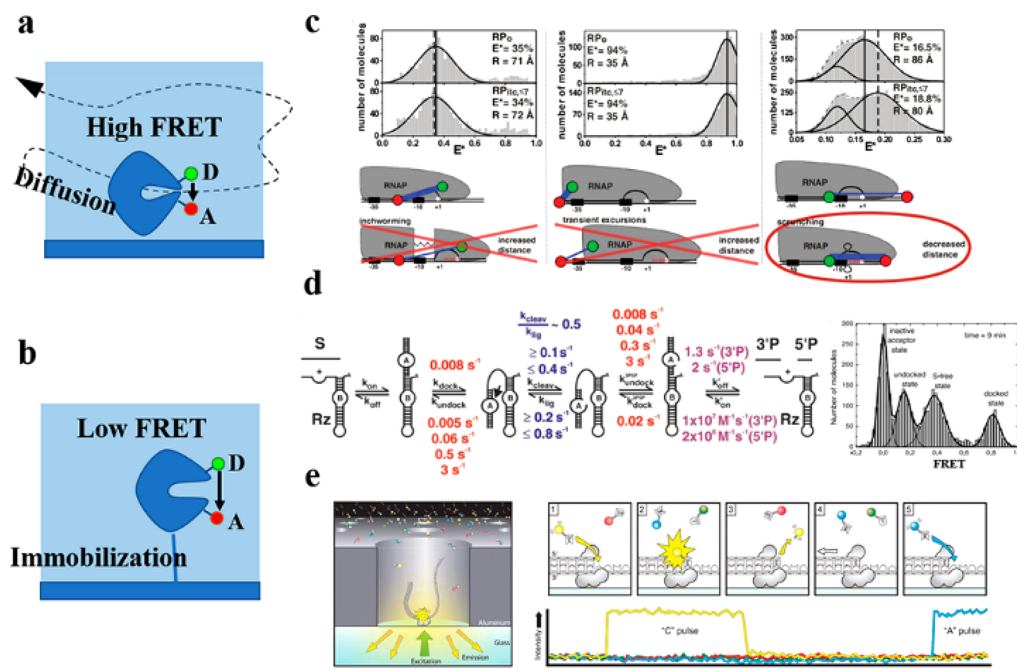


Figure 1. Methods based on smFRET rely on (a, b) diffusing and immobilized molecules. (b, d, e) Typical areas of smFRET investigations include (c) transcription initiation related to a DNA scrunching mechanism. Reproduced with permission from ref 76. Copyright 2018 AAAS. (d) Structural dynamics of ribozymes. Reproduced with permission from ref 18. Copyright 2018 AAAS. (e) Confined DNA sequencing. Reproduced with permission from ref 92. Copyright 2009 AAAS.

excited state. Electron relaxation quenches donor fluorescence emission by energy transfer, which results in fluorescence of the acceptor. Förster and Oppenheimer⁷⁶ proposed and quantified the rate of energy transfer (E_{FRET}), which is dependent on the distance between donors and acceptors to the sixth power:

$$E_{\text{FRET}} = \frac{1}{1 + (R/R_0)^6}$$

wherein R/R_0 is the ratio of the distance between the centers of the donor and acceptor molecules and the characteristic distance at which half of the donor energy is transferred to the acceptor. E_{FRET} enables the changes in distance between donors and acceptors to be determined over the course of an experiment. Chromosphere sites can be used to record and analyze simultaneous blinking of donors and acceptors at the single-molecule level, allowing FRET to elucidate conformational- or dynamic-processes or the relative positions of two biomolecules. Since the publication of the first FRET demonstration at the single-molecular level in 1996,⁷⁷ a series of complex biological systems have been studied using FRET. In this section, we focus on the latest single-molecule FRET (smFRET) technologies, which are divided into three categories (Figure 1): free diffusion, immobilized molecules, and restricted molecules.

2.1.1.1. Freely Diffusing Molecules: Transcription Initiation. Diffusion-based smFRET can be used to probe the molecular heterogeneity of freely diffusing molecules in aqueous conditions using confocal microscopy (Figure 1a).^{78–80} Since its first report, smFRET has been widely used to investigate protein folding,^{13,79} transcription initiation,⁸¹ and protein rotation.⁸² Transcription initiation is a well-known concept; however, its three molecular mechanisms (transient excursions, inchworming, and scrunching) have long

been disputed due to insufficient experimental evidence at the single-molecular level. The “inchworming” mechanism hypothesizes the expansion and contraction of RNA polymerase (RNAP), “transient excursions” describes the movement of the trailing edge of RNAP relative to DNA, and “scrunching” describes the expansion and contraction of DNA. The “scrunching” mechanism was identified using distinct labeling schemes (Figure 1c).⁸¹ FRET signals of the RNAP-promoter open complex (RPo) and RNAP-promoter initial transcribing complex (RPitc) showed no expansion or contraction of RNAP or movement of the trailing edge of RNAP relative to DNA.⁸³ In addition, their results directly verified the “scrunching” mechanism, wherein DNA searched and was fixed onto the active site by the compaction and unwinding stresses, thus ruling out the possibility of the “inchworming” and “transient excursion” mechanisms.

2.1.1.2. Immobilized Molecules: Ribozyme and Translation Initiation. Many biochemical functions occur on the millisecond or second time scale. To observe individual molecules over a longer period of time (up to minutes), immobilized smFRET was developed, which tethers the biomolecule onto a surface. This allows kinetic rates to be investigated by extracting data from histograms of dwell times in the distinguishing states (Figure 1b).^{5,84} Ribozyme molecules are a class of RNA molecules that display catalytic activity that depends on whether their folded structures are present in either the active (docked) or inactive (undocked) states. To study the relationship between the folding structures of ribozymes and their catalytic function, Zhuang et al.¹⁸ used 3' and 5' ends of hairpin ribozymes as fluorescent dyes to study the structural dynamics using smFRET. The dyes are tethered to the surface by biotin that is attached to the 5' end of the ribozyme. The cleavage activity of the immobilized ribozyme of interest was then determined and revealed four stable intermediate states (Figure 1d). By studying the

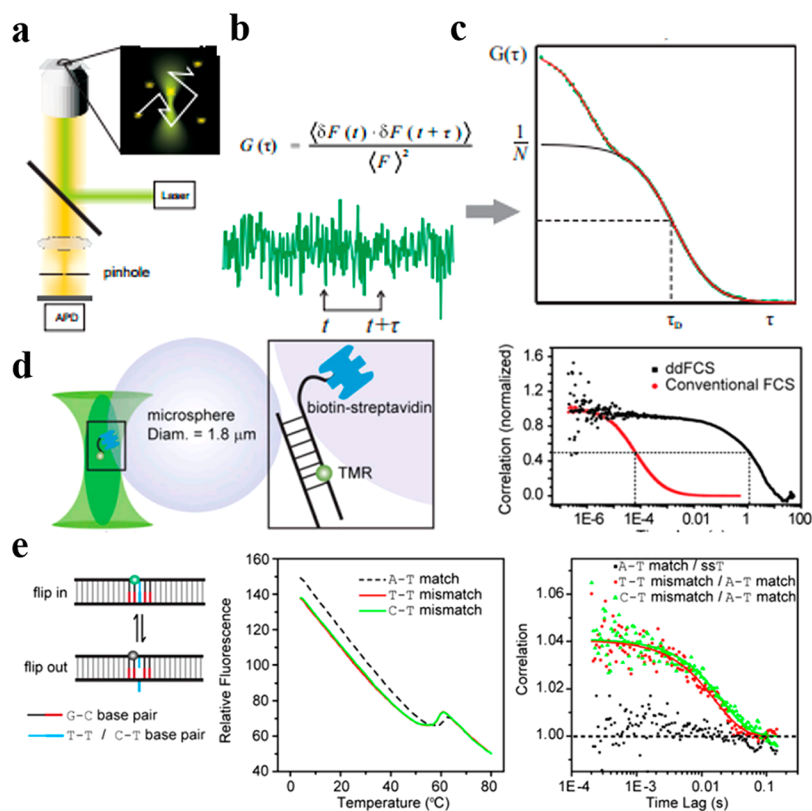


Figure 2. Principle of smFCS: (a) illustration of the smFCS detection strategy, (b) fluorescent intensity fluctuations of molecules diffusing through the detection volume, and the (c) correlation curve. Reproduced with permission from ref 101. Copyright 2012 John Wiley and Sons, Inc. Typical examples of smFCS studies include: (d) spontaneous flipping dynamics and (e) spontaneous flipping of the mismatched T–T and C–T base pairs. Reproduced with permission from ref 113. Copyright 2014 National Academy of Sciences.

conformational changes of ribozyme binding to substrates, direct evidence shows that cleavage occurs only in the active state (Figure 1d). Surface-immobilized FRET enables expansive superior experimental timeframes to investigate biological dynamic processes, enabling the study of longer biological functions such as nucleic acid conformational dynamics,^{85–87} protein activity,^{88–90} and protein folding.⁹¹

2.1.1.3. Confined Molecules: DNA Sequencing. Molecule-confined smFRET uses diffusion and surface immobilization to confine freely diffusing molecules within limited nanocontainers. Currently, zero-mode waveguide (ZMW),^{92,93} vesicle encapsulation,⁹⁴ and porous vesicles⁹⁵ are applied as nanocontainers to investigate dynamic biomolecular processes. Figure 1e presents the real-time, single-molecule detection of DNA sequencing.⁹² Here, a DNA polymerase was tethered to the ZMW, and four fluorescently labeled deoxyribonucleoside triphosphates (dNTPs) were used to perform an uninterrupted, template-directed synthesis (Figure 1e). The ZMW array allows real-time observation and detection of single-molecule fluctuations in a high-throughput manner, enabling industrial applications.

2.1.2. Single-Molecule Fluorescence Correlation Spectroscopy (smFCS). Instead of imaging the fluorescence of a single molecule, FCS analyzes fluctuations in the fluorescence intensity over time.^{96,97} With the development of techniques that reduce background signals using selective excitation strategies, fluorescence intensity fluctuations from a limited observation volume (usually $<10^{-15}$ L) can be obtained by TIRF⁹⁸ or single-plane illumination,⁹⁹ making it possible to track single molecules. Fluctuations in fluorescence, caused by

diffusion or chemical reactions of a luminescent probe labeled on the sample, can be tracked as biomolecules pass through the measurement volume (Figure 2a).^{100,101} In FCS, single photon arrival times (t) are detected by highly sensitive avalanche photo diodes (APDs) (Figure 2b). By fitting the fluorescence intensity $F(t)$ at time t to an autocorrelation function, an autocorrelation curve, $G(\tau)$, can be calculated (Figure 2c):¹⁰²

$$G(\tau) = \frac{\langle \delta F(t) \delta F(t + \tau) \rangle}{\langle F(t) \rangle^2}$$

where τ is the correlation time. The autocorrelation curve reflects the probability of being the same molecule at different times.¹⁰³ Dynamic parameters of the fluorescently labeled molecules can be discerned by fitting the autocorrelation curve with a suitable model function.²⁴ In contrast to smFRET measurements, smFCS is not limited to a detection size of 1–10 nm and is sensitive to distances shorter than 1 nm,^{104,105} making it applicable to a wide range of investigations in the biological sciences such as obtaining reaction rates, diffusion coefficients, and affinity constants.^{106–108}

2.1.2.1. One-Photon Excitation smFCS: Spontaneous Base Flipping. Spontaneous flipping of a single base in normal DNA is a fundamental issue in DNA biophysics.¹⁰⁹ The damaged base of normal Watson–Crick pairs is distinguished by spontaneous flipping of a mismatched or lesion base.¹¹⁰ It significantly impairs DNA–protein interactions during DNA repair or modification, in which proteins search and are fixed on the lesion or mismatched bases to modify the DNA, thereby maintaining genome integrity.^{111,112} Zhao et al.¹¹³ used smFCS to monitor the structural dynamics of spontaneous flipping of

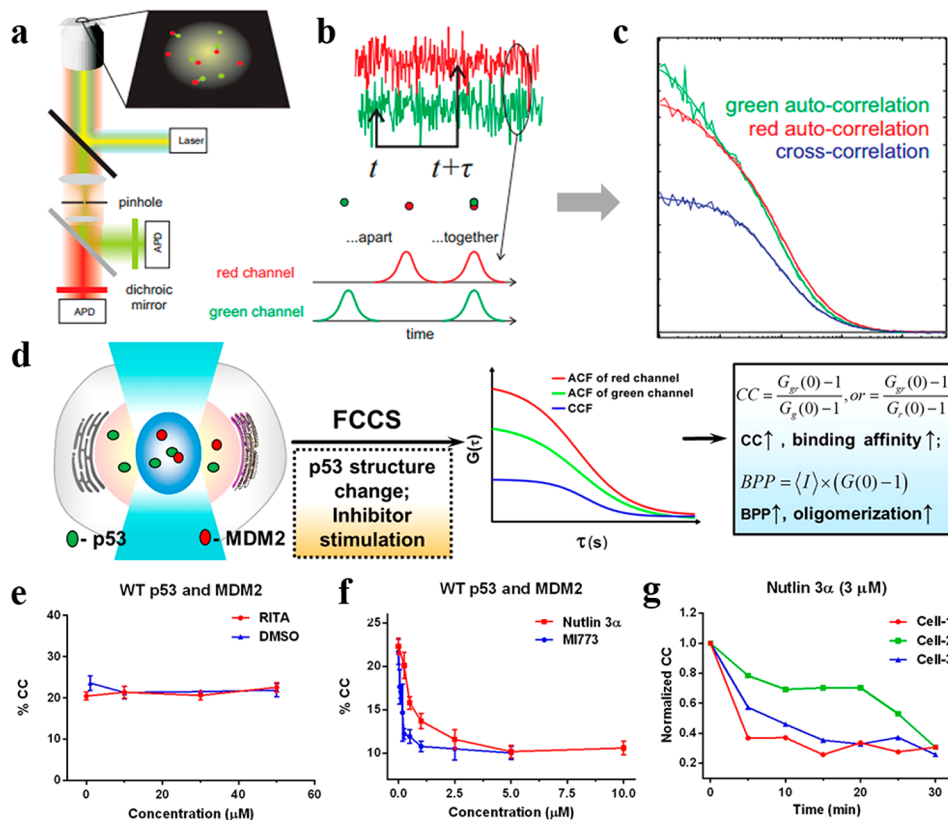


Figure 3. Principle of smFCCS: (a) illustration of the smFCCS detection strategy, (b) fluorescent intensity fluctuations of molecules diffusing through the detection volume, and (c) cross-correlation curves. Reproduced with permission from ref 101. Copyright 2012 John Wiley and Sons, Inc. Typical examples of smFCCS studies include: (d) quantification of the p53-MDM2 interaction, (e) effects of inhibitor (RITA) on the p53-MDM2 interaction compared to a DMSO control, (f) effects of inhibitors (Nutlin 3 α and MI773) on the p53-MDM2 interaction, and (g) dissociation kinetics of p53-MDM2 complexes in the presence of inhibitors. Reproduced with permission from ref 25. Copyright 2018 American Chemical Society.

mismatched bases in DNA duplexes. By using diffusion-decelerated smFCS (Figure 2d),^{114–116} in which polystyrene microspheres are attached to the double stranded DNA molecule to reduce the molecular rate, they observed that the base of a single mismatched or damaged base pair in double stranded DNA can be spontaneously excited out of the DNA duplex (Figure 2e). Relaxation lifetimes are on the order of 10 ms, four orders of magnitude slower than the lifetime obtained by nuclear magnetic resonance spectroscopy (NMR).^{117–119} The authors concluded that the spontaneous flipping rate obtained by NMR is most likely the base-wobbling rate rather than the flipping rate.

2.1.2.2. Dual-Color smFCCS: Protein–Protein Interactions.

It should be noted that the sensitivity of the autocorrelation analysis is limited because the diffusion coefficient also depends on the hydrodynamic radius of the molecule. To overcome the limitations of smFCS to study weight reaction partners (e.g., homodimers), dual-color fluorescence cross-correlation spectroscopy (FCCS, Figures 3a–c) was developed.¹⁰¹ Here, the intensity traces of two spectral channels are cross-correlated:

$$G_{rg}(\tau) = \frac{\langle \delta F_r(t) \delta F_g(t + \tau) \rangle}{\langle F_r(t) \rangle \langle F_g(t) \rangle}$$

wherein $F_g(t)$ and $F_r(t)$ are the intensities in the green and red channel, respectively. A positive contribution of the cross-correlation amplitude is observed when the two molecules of

interest interact and diffuse as a single molecule through the detection volume. Therefore, the degree of binding can be quantified from the autocorrelation curves (the green and red channels) and the amplitude of the cross-correlation curve $G_{rg}(\tau)$. First reported by Eigen and Rigler,¹²⁰ the concept of FCCS was experimentally demonstrated in the study of the annealing structural dynamics of two distinguishing labeled ssDNA strands. FCCS was successfully applied *in vitro* and *in vivo* to investigate enzymatic cleavage¹²¹ and protein aggregation¹²² during the endocytosis of cholera toxin.¹²³ Ren et al.²⁵ quantitatively examined the interaction between protein 53 (p53) and MDM2 and the dissociation kinetics of p53-MDM2 complex in living cells using smFCCS. The p53 and MDM2 proteins were labeled with enhanced green fluorescent protein (EGFP, green) and mCherry (red), respectively, and two fluorescent signal fluctuation channels were recorded to obtain the autocorrelation curve function (ACF) and cross-correlation curve function (CCF) (Figure 3d). The effect of some inhibitors (Nutlin 3 α , MI-773 and RITA) on the interaction of p53-MDM2 in DMSO was studied by FCCS (Figure 3f). DMSO and RITA did not inhibit the interaction of p53-MDM2 (Figure 3e). In contrast, the binding affinity of p53 to MDM2 decreased significantly with the increase of Nutlin 3 α and MI-773 concentrations (Figure 3f). Dissociation kinetics of p53-MDM2 complex was determined by recording single living cell in real time (Figure 3g). With the prolongation of incubation time, the dissociation degree of p53-MDM2 decreased significantly.

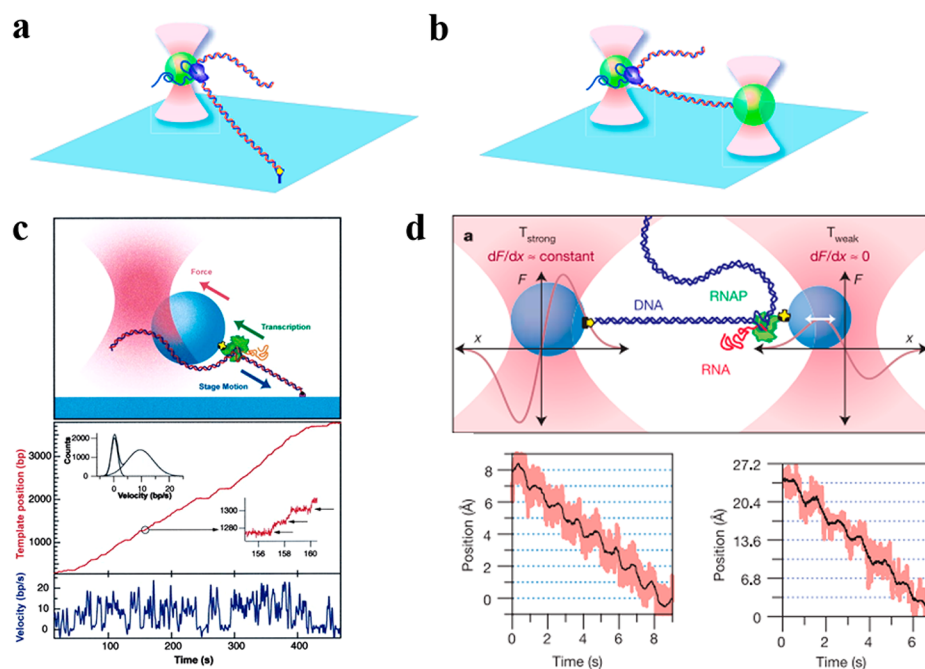


Figure 4. Methods based on single-molecule optical tweezers: (a) the tethered assay and (b) dumbbell assay. Reproduced with permission from ref 130. Copyright 2008 Springer Nature. Typical examples of single-molecule optical tweezer studies include: (c) dynamics of pauses in transcription extension (reproduced with permission from ref 30. Copyright 2003 Elsevier) and (d) dynamics of RNAP advancing along DNA in transcription extension. Reproduced with permission from ref 26. Copyright 2005 Nature Publishing Group.

2.2. Single-Molecule Force Techniques. **2.2.1. Optical Tweezers.** An optical tweezer, known as an optical trap,¹²⁴ is the most well-known single-molecule manipulation technique. An optical trap can be created by focusing a laser on a diffraction limited spot.¹²⁵ When the sample of interest is labeled by micron- or nanosized plastic beads, the beads are trapped at the focus of the optical trap that is used to control the position of the sample. Dielectric particles near the focus point experience a three-dimensional restoring force that directs the molecule to the focus point. Therefore, the optical trap serves as a spring, which produces a restoring force: the force that brings the beads back to the center of the trap. The restoring force grows linearly with the plastic bead's distance from the central optical trap.²¹ Therefore, the micron-sized polystyrene beads can serve as handles to manipulate the molecule on which they are attached. This technology can apply more than 0.1–100 pN force on the beads, measuring the three-dimensional displacement of the captured beads with sub nanometer precision and sub millisecond time resolution, making the optical tweezers an ideal tool for measuring force and motion.¹²⁶ Currently, optical tweezers have been used to explore the mechanics of biological events such as the motion of molecular motors,¹²⁷ protein and nucleic acid folding and unfolding,^{26,128} and transition-state analysis.¹²⁹ There are two classes of optical tweezer assays: tethered and dumbbell assays.¹³⁰ In tethered assays, a bead is labeled on the biomolecule of interest that is immobilized on a substrate. An optical trap is then used as a force and displacement transducer (Figure 4a). The dumbbell assay is similar to the tethered assay, but the dumbbell assay employs a second bead that is attached to the other end of the biomolecule. A second optical trap is then used as force and displacement transducer (Figure 4b). A dramatic reduction in noise and drift can be achieved in dumbbell assays because both beads are suspended in solution.

2.2.1.1. Tethered Assay: Transcription Extension. Periods of nucleotide addition are interrupted with frequent pauses that make the RNAP transcribe discontinuously. One pause mechanism is related to the paused conformation of RNAP. It is hypothesized that the pause is caused by a rearrangement of the RNAP active site. A second type of pause, a “backtracking” pause, is related to the backward movement of RNAP along the DNA and RNA strands. Block et al. reported the single-molecule optical trapping experimental evidence of characterization of the mechanism of pausing during transcription (Figure 4c).³⁰ An effect of conformational transitions on the rate and equilibrium constants was observed when a force was applied when RNAP was moving backward. The results demonstrated that neither the rate nor the equilibrium constants of these ubiquitous pauses in transcription was affected by hindering or assisting loads, suggesting that these ubiquitous pauses are not caused by RNAP backtracking on the DNA template. Instead, the authors assigned these results to the structural rearrangement within the enzyme.

2.2.1.2. Dumbbell Assay: Transcription Extension. During transcription, DNA replication and repair requires the formation of protein–DNA complexes and persistent movement of proteins along the DNA strand. Therefore, the interaction forces between proteins and DNAs often utilize intermolecular interactions. Block et al.²⁶ directly observed the continuous movement of RNAP along a DNA template during the creation of a complementary RNA strand by single-molecule optical tweezer nanotechnology (Figure 4d). The authors fixed polystyrene nanobeads on the DNA template chain and RNAP molecule. When RNAP adhered to the DNA strand and began to synthesize RNA along the template chain, the DNA strand between the beads elongated, which caused the two beads to separate. The results revealed that each discrete step is approximately 3.7 ± 0.6 Å. This distance is equal to the average length of each DNA base. This result is

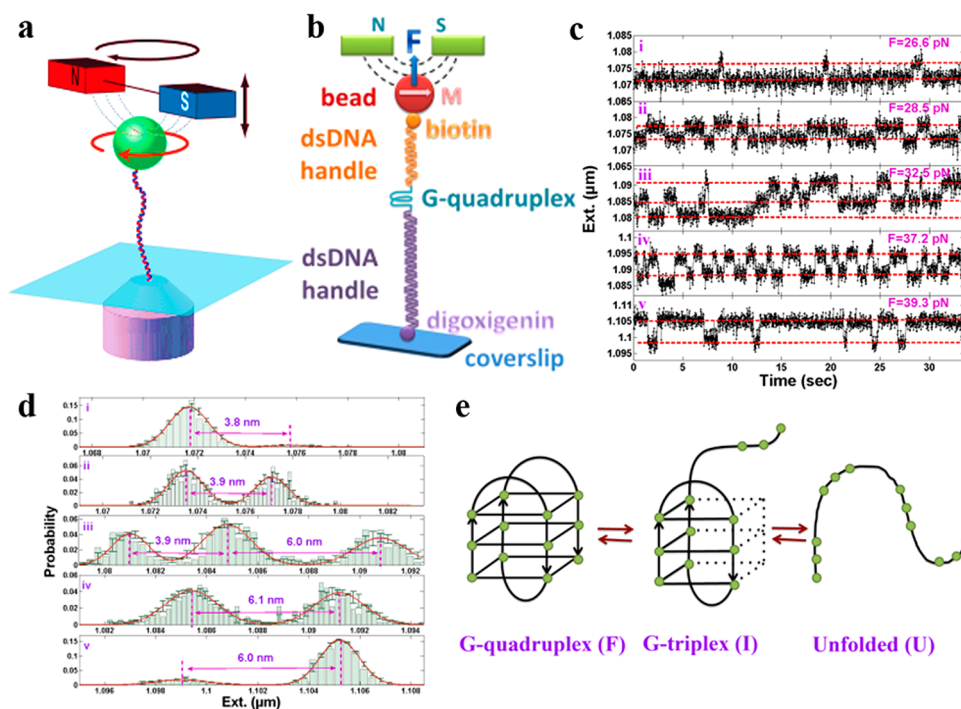


Figure 5. Magnetic tweezer-based biosensors. (a) Principle of single-molecule magnetic tweezers. Typical examples of single-molecule magnetic tweezer studies include: (b) dynamics of the folding pathway of single human telomeric G-quadruplexes. Reproduced with permission from ref 130. Copyright 2008 Springer Nature. (c) Sequential unfolding trajectories of the G-quadruplex under different constant tensions, (d) probability distributions of the extension under different tensions, that correspond to the trajectory c, and (e) model proposed to explain the sequential unfolding pathway of the G-quadruplex. Reproduced with permission from ref 31. Copyright 2013 American Chemical Society.

direct evidence that RNAP advances along DNA by one base pair when a new base pair nucleotide is added to the nascent RNA strand. Recently, Shrestha et al. employed optical tweezers to explore the pure effect of confined space on the property of individual human telomeric DNA G-quadruplexes by using DNA origami nanocages.¹³¹

2.2.2. Magnetic Tweezers. The concept of magnetic tweezers is similar to that of optical tweezers; a small magnetic particle is controlled by permanent magnets.^{128,130} Magnetic tweezers enable a force to be applied on the biomolecule that is labeled with a magnetic particle. In contrast to optical tweezers, a twisting force can easily be applied with magnetic tweezers. This approach is particularly useful for studying high-level structural properties of DNA, such as the dynamics of the DNA double helix structure¹³² and G-quadruplex structures.³¹

Unprecedented control over DNA topography can be obtained with magnetic tweezers, enabling delicate measurements of the topoisomerase activity at the single-molecule level. For instance, Li et al. used magnetic tweezers to directly measure the folding pathway of single human telomeric G-quadruplexes.³¹ One end of the DNA was anchored to a magnetic bead, while the other end was adhered to a glass coverslip (Figure 5b). Under different tensions, the G-quadruplex exhibited multiple unfolding states (Figure 5c,d). The intermediates, G-triplex, of the G-quadruplex unfolding process were obtained by fine-tuning the force exerted on the DNA and recording the end-to-end extension (Figure 5e). These data unambiguously supported a sequential folding model of the G-quadruplex and resolved the debate regarding the G-quadruplex folding pathway.

3. LABEL-FREE SINGLE-MOLECULE NANOTECHNOLOGIES

Labeled single-molecule detection strategies have primarily been employed in single-biomolecule detection. However, sufficient temporal resolution remains a challenge at the single-molecule level. Label-free, real-time, and highly sensitive single-molecule detection techniques can reveal molecular heterogeneity during the dynamic behavior of individual biomolecules.

3.1. Single-Molecule Optical Methods. **3.1.1. Ultrafast Spectroscopy.** Since Maiman reported the first stimulated optical radiation in ruby in 1960, the development of nonlinear optics has significantly impacted the study and understanding of biological systems.¹³³ Ultrafast spectroscopy can be used to investigate dynamic processes at the single-molecule level. This technique uses a pump–probe (PP) or two-dimensional electronic spectroscopy (2DES) to successively record changes in the target environment over time. In brief, an initial pump pulse excites the molecule of interest and a second pulse probes, which creates a recording signal as a function of dwell-time delay between pump and probe pulses. In addition, 2DES resolves the detected signal as a function of excitation energy, directly measuring multiple transitions, which prevents the problem of untangling overlapping signals.

The photoinduced activity of light harvesting biosystems has drawn significant attention from the scientific community. Four decades ago, the first high-resolution structural information of the Fenna-Matthews-Olson (FMO) complex was clarified, the light-harvesting (LH) processes of photosynthetic pigment–protein complexes has been an active area of investigation. In 2005, Fleming and his co-worker obtained the 2DES of the antenna FMO bacteriochlorophyll, a (BChl)

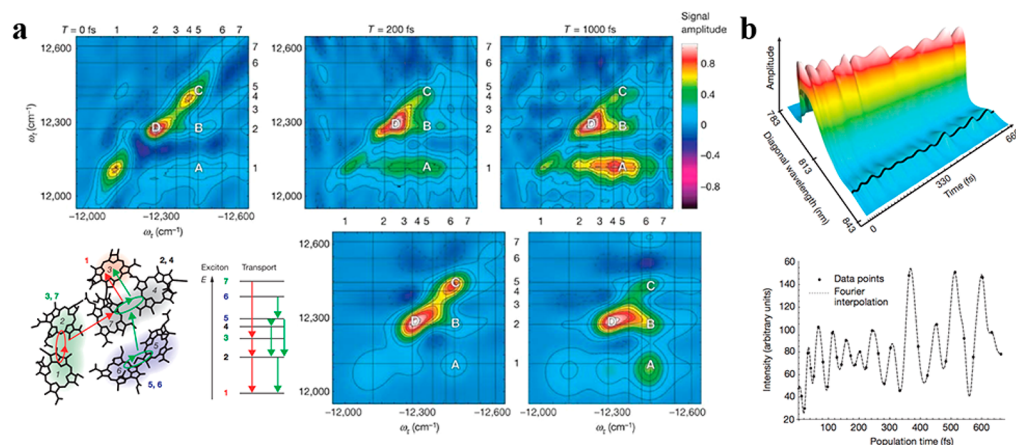


Figure 6. 2DES of FMO complexes. (a) Experimental and theoretical spectra (real parts) from *Chlorobium tepidum*. Reproduced with permission from ref 37. Copyright 2005 Nature Publishing Group. (b) Data showing electronic coherence beating at 77 K. Reproduced with permission from ref 38. Copyright 2007 Springer Nature.

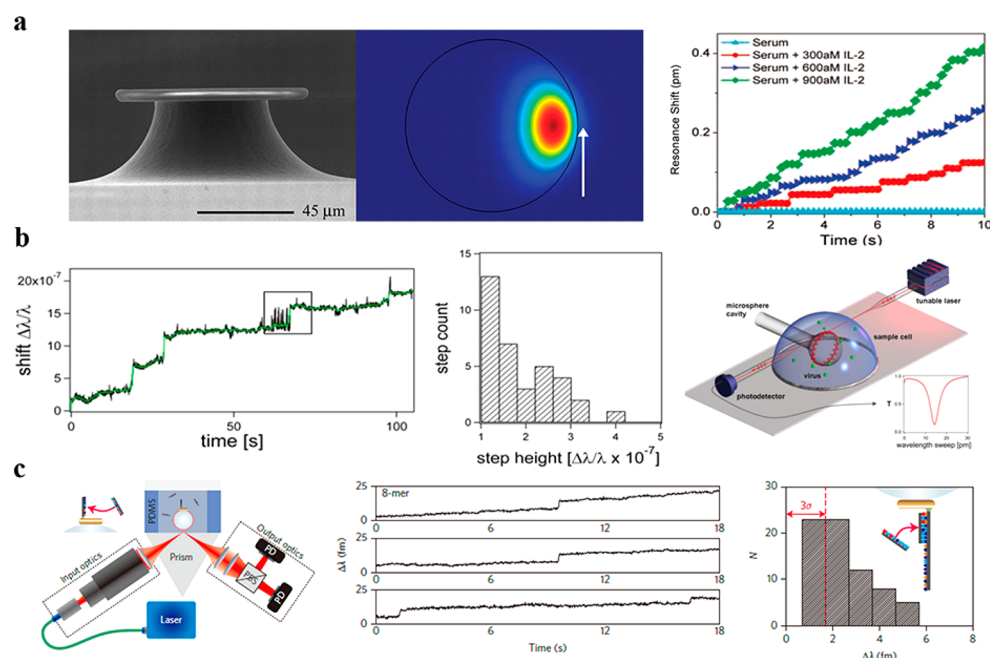


Figure 7. Methods based on WGM include: (a) single-molecule detection of interleukin-2 in serum. Reproduced with permission from ref 41. Copyright 2007 AAAS. (b) Influenza A single virus detection. Reproduced with permission from ref 144. Copyright 2008 National Academy of Sciences, and (c) monitoring single-molecule nucleic acid interactions on the microcavity biosensor platform. Reproduced with permission from ref 40. Copyright 2014 Nature Publishing Group.

protein from green sulfur bacteria (Figure 6a). Their results revealed that two energy transfer pathways coexist in FMO complexes that contribute to the light harvest process.³⁷ However, in 2007, the same group observed a quantum beating that lasted for 660 fs, and with growing evidence of wave-like energy transfer in the FMO complex (Figure 6b),^{38,39} the scientists revised their mechanism for energy transfer in the FMO complex to that of quantum coherences. Analogous mechanisms have been verified in other light harvesting systems, such as cryptophyte phycobiliproteins, PE545 complexes from *Rhodomonas* CS24, PC645 complexes of the alga *Chroococcus* CCMP270,^{134,135} light harvesting complex II (LHCII),¹³⁶ bacterial reaction center,¹³⁷ and photosystem II (PS-II).¹³⁸

3.1.2. Optical Microcavity Based on Whispering Gallery Mode (WGM). As a label-free and highly sensitive optical

transducer, microcavity sensing attracts significant attention with broad applications including environmental dynamic processes,^{139,140} clinical diagnostics,¹⁴¹ and nanoparticle and single virus detection.^{142,143} The resonant recirculation of light within the microcavity enables the light to sample the molecules of interest multiple times. This provides an ultrahigh Q factor (10^8) and small mode volumes, significantly enhancing light–matter interactions.⁴¹

Microcavity single-molecule detection enables the observation of individual molecular binding events that shift the resonant frequency, resulting from a thermooptic mechanism, and subsequently statistically confirms these shifts over several binding events. Figure 7 illustrates various WGM cavity geometries and materials for versatile targeting of single-molecule detection. A planar array of functionalized silica microtoroid WGM has been used to investigate individual

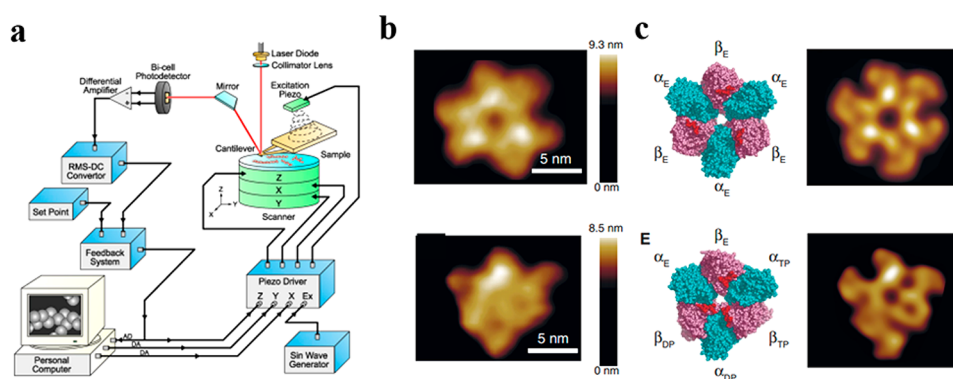


Figure 8. AFM-based single-molecule techniques. (a) Components and typical instrumentation of AFM is shown. Reproduced with permission from ref 146. Copyright 2013 American Chemical Society. (b, c) Typical examples of HS-AFM studies include the structural dynamics of ATP hydrolysis by the F1-ATP enzyme. Reproduced with permission from ref 42. Copyright 2011 AAAS.

human interleukin-2 (IL-2) molecules in serum with a mode-locking technique (Figure 7a).⁴¹ The binding of IL-2 to microtoroid created a stepwise resonant frequency shift. A single nanoparticle detection measurement was reported with the WGM of a microsphere, in which individual discrete binding events of the Influenza A viruses were performed by scanning resonance wavelength with tunable laser (Figure 7b).¹⁴⁴ The limit of detection was improved to a mass of approximately 2350 Da with plasmonic enhancements, which was demonstrated by the hybridization of 8-mer nucleic acid oligonucleotides in the microsphere WGM (Figure 7c).⁴⁰ These nanotechnologies enable WGM to be applied to a diverse set of applications and potentially be integrated on a chip.¹⁴³

3.2. Single-Molecule Mechanical Methods. In 1986, AFM was invented by Binnig et al.,¹⁴⁵ which is a force-based technique that scans the sample surface using the tip of a microcantilever to image and visualize structural information (Figure 8a).¹⁴⁶ A tip of atomic size can directly operate and image single molecules in physiologically relevant solutions, which was made possible by development of the tapping mode in 1993,¹⁴⁷ in which damage to the sample is avoided by maintaining a continuous tip-sample contact, and the in-liquid imaging method in 1987.¹⁴⁸ Despite the success of AFM in protein structure imaging, the slow scanning speed of traditional AFMs hinders the detailed study of protein structure dynamics. The scanning speed of commercial AFM instruments usually varies from a few seconds to a few minutes per frame, while biological reactions occur in the sub second level or even faster. The first generation of high speed (HS) AFM is developed by optimizing the cantilever, scanning stage, amplitude DC converter, and dynamic PID controller of AFM. The image acquisition speed is 12.5 frames/second.⁴² The development of HS-AFM is ongoing. At present, the HS-AFM instrument established in the laboratory can record a film with an imaging speed of about 33 frames/second and has a time and space resolution suitable for dynamic analysis of biological samples.^{149,150}

DNA-enzyme reactions are the most common biochemical reactions in cells. Yokokawa et al.¹⁵¹ imaged the DNA cleavage reaction by a type IIP restriction endonuclease, ApaI, using a newly developed HS-AFM. From HS-AFM images obtained at different time points, it was discovered that ApaI binds to DNA in the form of dimer and slides along DNA in a one-dimensional diffusion manner. When it encounters a specific DNA sequence, the enzyme stops digesting the DNA. After

digestion, the ApaI dimers were immediately separated into two monomers, each of which remained at the end of DNA and then separated from the end of DNA. Noji et al.⁴² imaged the catalytic kinetic process of ATP hydrolysis by the F1-ATP enzyme. This is a classic example of molecular conformational transformation studies by HS-AFM. They used HS-AFM to scan the structure of F1-ATPase during the catalytic hydrolysis of ATP (Figure 8c) to obtain the whole rotational dynamics of the F1-ATPase. Their results demonstrated that the rotorless F1 continuously “rotates”; the $\beta 3$ subunits circulate in a counterclockwise direction, similar to the rotation of the axis of rotation in F1, in the $\alpha 3\beta 3$ stator ring. HS-AFM is a powerful tool that can be used to explore the structural dynamics of biomolecules on the subsecond time scale and the single-molecule level.

3.3. Single-Molecule Electrical Detection. **3.3.1. Carbon Nanotube- and Silicon Nanowire-Based Single-Molecule Electrical Detection.** Carbon nanotubes (CNTs) and silicon nanowires (SiNWs) enable robust, thermally stable, and covalent-based electrical detection by providing a sufficiently large area to permit both spectroscopic monitoring and microelectronics integration, making them a reliable platform for more complicated biological measurements.

3.3.1.1. SWCNT-Based Single-Molecule Electrical Detection. Single-wall carbon nanotubes (SWCNTs) are one of the most well-known one-dimensional materials since their initial reporting in 1991.¹⁵² SWCNTs provide the requisite bandwidth and sensitivity to detect and monitor single-molecular dynamics. CNTs have been employed in a variety of nanoelectronics such as field-effect transistors (FETs), logic gates, memory devices, and optoelectronic detectors and sensors.¹⁵³ Additionally, SWCNTs are biocompatible due to their nanoscale diameter and ability to be easily functionalized.^{154–156} In particular, prominent and tunable electrical properties and large specific surface area make CNTs a promising bioelectronic sensor. Strong C–C σ bond and delocalized π electrons throughout the surface make the SWCNTs electrically conductive. In principle, molecules of interest may be tethered directly to a CNT-FET. The CNT-FET is then able to accept a biological signal from the target molecule and convert it into electrical signals by changing the conductivity of the FET.

3.3.1.2. π - π Stacking: Enzymatic Activity. Rather than introducing a point defect, tailoring its chemistry, and then conjugating a molecule of interest to the functionalized site, a noncovalent bioconjugation strategy was introduced by Philip

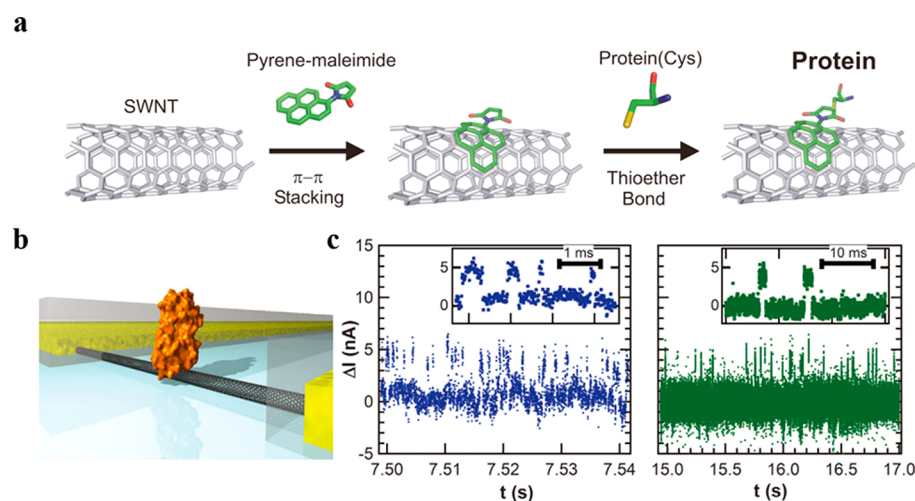


Figure 9. SWCNT-FET-based single-molecule detection technique. (a) Illustration of the strategy used to adhere biomolecules and proteins onto the SWCNT via a pyrene–maleimide linker. Reproduced with permission from ref 157. Copyright 2013 American Chemical Society. (b) Illustration of a single lysozyme being interrogated by a SWCNT nanocircuit. The partial poly(methyl methacrylate) coating is depicted in gray. (c) Faster (blue) and slower (green) current oscillations. The insets show individual switching events for each case. Reproduced with permission from ref 44. Copyright 2012 AAAS.

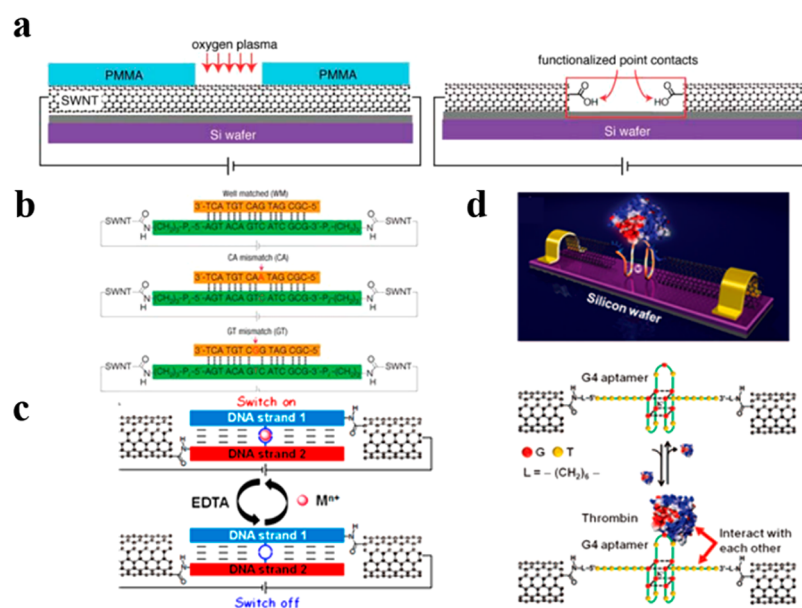


Figure 10. Methods based on SWCNT nanocircuits. (a) PMMA window template, defined with e-beam lithography, is used to precisely cut SWCNTs with oxygen plasma to create a molecular-scale gap. Reproduced with permission from ref 166. Copyright 2006 AAAS. (b) Illustration of SWCNTs functionalization with DNA strands in the molecular-scale gap. Reproduced with permission from ref 53. Copyright 2008 Nature Publishing Group. (c) Illustration of the sensing process of SWCNT-metallo-DNA junctions. Reproduced with permission from ref 54. Copyright 2011 John Wiley and Sons, Inc. (d) Illustration of SWCNT-DNA aptamer junctions, protein binding used to strengthen π stacking of G4 conformation, and the sensing mechanism for thrombin. Reproduced with permission from ref 48. Copyright 2011 John Wiley and Sons, Inc.

Collin's group in 2012.⁴⁴ They developed a noncovalent immobilization method based on pyrene linkers, which provides a low density of anchor points for subsequent derivatization of the nanotube surface (Figure 9A). Pyrene attaches to the SWCNT surface by engaging in π - π stacking.

This strategy was used to covalently conjugate a target protein to the pyrene-maleimide anchor site via a cysteine thiol. Figure 9a displays a single lysozyme interrogated by a carbon nanocircuit. AFM was used to confirm adhesion of the lysozyme onto the SWCNT surface (Figure 9b). By monitoring the $I(t)$ of the SWCNT-FET, they demonstrated the dynamics of a single T4 lysosome hydrolyzing a glycosidic

bond. Specifically, 100 glycosidic bonds are hydrolyzed successively at a 15-Hz rate before the lysozyme returns to its nonproductive 330-Hz hinge motion. Further statistical analysis indicated that the single-step hinge closure occurs in two steps. The authors used the same pyrene linker strategy to investigate the dynamics of the homopolymeric process of single DNA polymerase I (Klenow Fragment) and the single-molecule catalysis by cAMP-dependent Protein Kinase A.^{45,46}

3.3.1.3. Covalent Binding: Point Defect Effect and DNA Hybridization. Several methods to fabricate electrical detection platforms have been developed. Philip Collin has conducted pioneering work by electrochemically introducing a

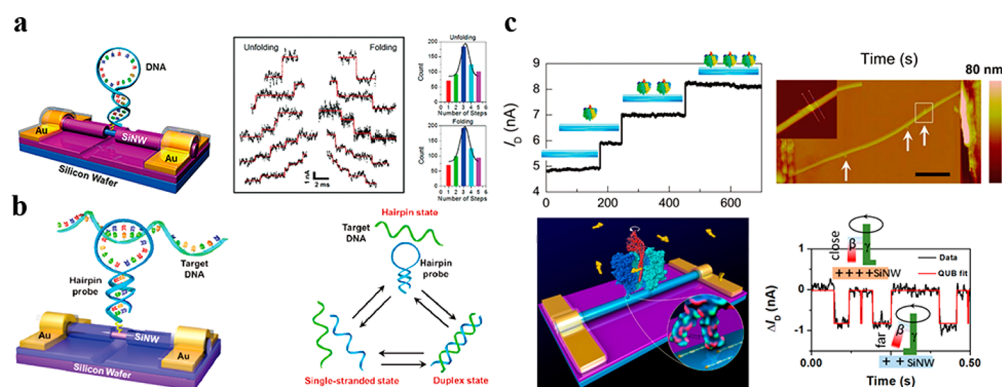


Figure 11. Methods based on SiNW nanocircuits. (a) Illustration of a single-hairpin DNA-decorated SiNW biosensors and its electrical measurement setup. Stepwise increases and decreases in the conductance are fitted by a step-finding algorithm (red), displaying the zero- to five-step growing and declining processes. Reproduced with permission from ref 51. Copyright 2016 John Wiley and Sons, Inc. (b) Illustration of a single-molecule biosensor with three-phase transitions during hairpin DNA hybridization of the complementary target. Reproduced with permission from ref 52. Copyright 2017 John Wiley and Sons, Inc. (c) Top: Dynamic process of F_1 -ATPase absorption/desorption, showing the gradual changes in I_D with three steps and the corresponding AFM images after protein delivery. Bottom: Dynamic processes of F_1 -ATPase molecular motor rotation. Reproduced with permission from refs 49 and 50. Copyright 2016 Royal Society of Chemistry and 2017 American Chemical Society.

point defect onto the CNT.^{44,46,157–159} The Shepard group fabricated a point-functionalized carbon nanotube surface using a similar method to that developed by Collin.¹⁶⁰ They covalently grafted a single stranded DNA probe to a carboxyl defect on the CNT surface and introduced a complementary target DNA segment. They were able to detect, in real-time, hybridization of the complementary DNA segment, which exhibited a two-level conductance fluctuation that depended on the temperature. By analyzing the melting curve, they attributed the low state to the double stranded DNA and the high state to the ssDNA. However, Debye screening of the single-molecule CNT-FET sensors made ssDNA hybridization/dehybridization indistinguishable from the intrinsic conductance change.¹⁶¹

To increase stability, a dash-line lithographic method was developed to precisely cut SWCNTs into nanocarbon electrodes with carboxylic acid end-groups, imparting a covalent binding site to confine the molecules of interest in the nanogap (Figure 10a).^{162,34} A molecular-scale gap was introduced onto SWCNTs by first creating a template window that is less than 10 nm in a spin-cast PMMA layer by ultrahigh-resolution electron beam lithography (EBL). Oxygen plasma ion etching is then conducted through the PMMA window to cut through the CNT to create molecular-scale gaps, which can be tuned to precisely fit the target molecule, that display carboxylic acid end-groups. Finally, the molecule of interest bridges the nanogaps and covalently adheres to the CNT through an amine functionality, which can be confirmed by inelastic electron tunneling spectroscopy (IETS).¹⁶³ The robust covalent-bond and confined space imparts superior stability to the SWCNT-FET devices. By leveraging the carboxylic acid end-group in SWCNTs, we developed pH sensors,¹⁶² reversible optical switches,^{163,164} and chemo-responsive monolayer transistors.¹⁶²

The unclear compatibility of DNA with electrical circuits has made the determination of charge transport properties difficult.¹⁶⁵ Accordingly, we bridged the DNA duplex in a CNT gap by the aforementioned method and monitored the current of the junctions as a function of time. Our results demonstrated that these devices are capable of distinguishing the fully bridged complementary DNA and those with a DNA

mismatch (Figure 10b).⁵³ In addition, introducing metal ions inside the DNA core increased the conductance of the junction, as it strengthened the π -stacking between base pairs (Figure 10c).⁵⁴ For more practical applications, we developed a biosensor to specifically detect thrombin by incorporating a G4 conformational single stranded DNA aptamer (Figure 10d).⁴⁸

3.3.2. SiNW-FET-Based Biosensor. A reliable biosensor requires (1) transduction of the biological event into electrical signals, (2) controllable chemical and electrical properties, (3) superior stability, (4) biocompatibility, and (5) compatibility with current silicon-based semiconductors and photovoltaics. Silicon-based circuits meet all of the above requirements and are becoming more prominent in our daily life. However, the monocrystalline silicon-based semiconductor does not satisfy Moore's law, motivating a switch to silicon nanowires (SiNWs).

3.3.2.1. Surface Functionalization: Single Virus Detection. The Lieber group first reported the direct, real-time electrical detection of single virus particles with highly selective SiNWs-FETs.¹⁶⁷ The SiNW surface was modified with antibody receptors to virus particles, enabling a change in conductance upon antibody engagement. This strategy has been further used for real-time detection of influenza H3N2 and H1N1 viruses from human exhaled breath condensate.¹⁶⁸

3.3.2.2. Point Functionalization: DNA Hybridization and Molecular Motor Rotation. A precise high-resolution EBL technique was used to determine the multiple adsorption sites on the SiNW surface. Subsequently, point functionalization was used to modify the SiNWs surface with various single molecular probes.¹⁶⁹ A DNA hairpin segment was incorporated onto SiNWs through the active ester terminals, with precise control over the measurement temperature between 20 and 65 °C at a 5 °C interval. The stepwise current revealed the dynamics of the unfolding/folding processes of the DNA hairpin hybridization (Figure 11a).⁵¹ This was the first time DNA hybridization was observed at the single-base level. Furthermore, a single hairpin DNA was incorporated as a molecular probe to create a low-cost, high-throughput, simple, and accurate single nucleotide polymorphism (SNP) genotyping technique (Figure 11b).⁵²

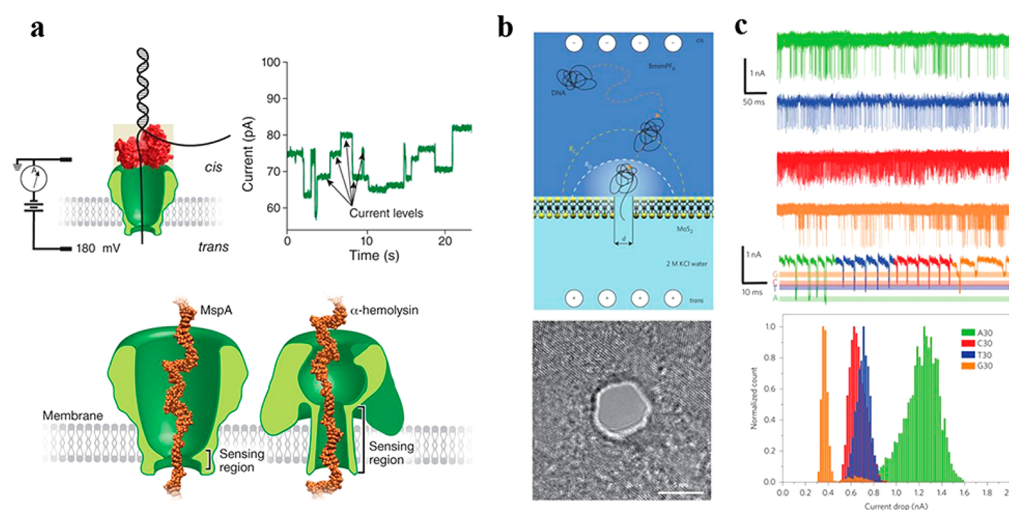


Figure 12. Nanopore-based biosensors. (a) Illustration of a protein-based nanopore used for DNA sequencing. Reproduced with permission from ref 56. Copyright 2016 Nature Publishing Group. (b) Illustration and characterization of the RTILs/KCl viscosity gradient system that is used in MoS₂ nanopores. (c) Differentiation of 30-mer oligonucleotides in a MoS₂ nanopore. Reproduced with permission from ref 170. Copyright 2015 Nature Publishing Group.

The dynamic processes of F₁-ATPase molecular motor rotation have been investigated by point functionalized SiNW biosensors.^{49,50} Functionalized Ni-NTA end groups were displayed on the SiNWs surface, which served as the selective binding sites for F₁-ATPase (F₁).⁴⁹ With real-time recording and AFM monitoring, the stepwise signal of His-tag F₁ adsorption was confirmed (Figure 11c). Subsequently, the addition of ATP resulted in a reproducible bistable conductance fluctuation, which stemmed from the binary configurational transition of the γ shaft of F₁ that corresponds to ATP hydrolysis and Pi release. The rate of label-free F₁ hydrolysis obtained was one order of magnitude higher ($1.69 \times 10^8 \text{ M}^{-1} \text{ s}^{-1}$ at 20 °C) than that determined from fluorescently labeled F₁, demonstrating the capability of SiNW-based electrical nanocircuits to nondestructively probe the intrinsic dynamics of biological activities.

3.3.3. Nanopore-Based Single-Molecule Electrical Detection. Significant attention has been given to nanopores due to their application in DNA sequencing.^{55,56} In the nanopore sequencing technique, the nanopores function as a biosensor and enable passage as the membrane contacts the ionic solution on both the *cis* and *trans* sides.⁵⁶ The chambers are filled with an ionic solution and are separated by a voltage-biased membrane (Figure 12a). Single strand polynucleotide (black) is driven by protein nanopore (green) electrophoresis, which provides the only path for ions or biomolecules to move from *cis* to *trans* chambers. Besides, the translocation of the target polynucleotide through the nanopore is controlled by an enzyme (red). The ion current through the nanopore was recorded by a sensitive galvanometer. The constant bias voltage drives the DNA through the nanopore, which results in a change of the ion current (Figure 12a). Only individual DNA molecules can pass through the nanopore, and theoretically, the ion current can distinguish differences in nucleotides A, T, C, and G. This motivates further investigations using nanopores for DNA sequencing technologies. Currently, only biological and solid-state nanopores are used in DNA sequencing.

3.3.3.1. Protein-Based Nanopores. The α -hemolysin pore was independently reported by Deamer and Branton as the

first nanopore, which is now considered to be a well-established nanopore.^{171,172} α -Hemolysin is a heptameric protein, which has a channel composed of a vestibule connected to a transmembrane β -barrel. Specifically, the β -barrel is approximately 2.6 nm in width and 5 nm in length and functions as the sensing region. It should be noted that the entrance of the β -barrel is 1.4 nm, which allows only one single stranded DNA polymer to go through at a given time. Deamer and Branton's work demonstrated the feasibility of the α -hemolysin nanopore in DNA sequencing.^{171,172} Subsequent experiments confirmed that blockade signals can be utilized to distinguish the purine and pyrimidine segments.¹⁷¹ Break-through sequencing using α -hemolysin was first reported by Bayley and Ghadiri. Their results indicated that a single adenine nucleotide differs from cytosines by its ion conductance.¹⁷³ Further experimental evidence supported their conclusion and demonstrated that all four DNA nucleobases can be differentiated from each other.¹⁷⁴ The biological nanopore sequencing landscape is thus dominated by α -hemolysin. However, the vestibule can only accommodate up to 10 nucleotides at a time with significant modulation of the ion current.¹⁷⁴ Structural challenges of the target protein can also reduce the overall signal-to-noise ratio, severely limiting its use in sequencing applications.

An octameric protein channel, MspA, has been genetically engineered with a tapered funnel shaped channel, which overcomes the signal-to-noise ratio challenge in α -hemolysin. The channel is 0.5 nm in length and 1.2 nm in diameter, which is much smaller than that of α -hemolysin. MspA has the potential to improve sequencing resolution; however, precise control of DNA translocation remains a central challenge with this method. Recently, the MspA nanopores have been used in sequencing mutagenic DNA lesions based on the quadromer map.^{177,178} Akeson and Gundlach introduced the phi29 DNA polymerase (phi29 DNAP) to accurately control DNA translocation. Their results showed comparable single-base resolution of DNA sequencing to that of MspA.^{175,176}

3.3.3.2. Solid-State Nanopores. As an alternative to biological nanopores, the robustness and durability of solid-state nanopores enable physical characteristics to be tuned

with subnanometer precision. Additionally, the high-density arrays of solid-state nanopores and their superior chemical, thermal, and mechanical properties enables integration with nanocircuits.^{179,180} In 2001, Golovchenko and his colleagues fabricated a Si₃N₄ nanopore with the focused ion beam (FIB) technique.¹⁸¹ The fabricated nanopore was the first solid-state nanopore reported to sense DNA. The most commonly used tool for nanopore sculpting is the focused electron beam, wherein a probe is used to sputter nanopores in thin insulating membranes.⁵⁵ Materials used for nanopores include: Si₃N₄, Si, SiO₂, Al₂O₃, and HfO₂.

Initially, solid-state nanopores could not offer single-base resolution in DNA sequencing due to challenges in fabricating precise nanopore sizes. Golovchenko, Johnson, and Dekker developed a graphene-based nanopore that combines the stability of the nanopore with a thickness comparable to ssDNA.^{182–184} Recently, Radenovic et al. used a single layer of MoS₂ to fabricate a nanopore and demonstrated the feasibility of DNA sequencing by a solid-state nanopore (Figure 12b).¹⁷⁰ They used a viscosity gradient system by employing room-temperature ionic liquids (RTILs), which imparts a high degree of freedom to temporal resolution by markedly slowing down DNA translocation, while exhibiting good ionic conductivity. Their nanopore system enabled electrical detection with single-base resolution and demonstrated the ability to distinguish four nucleotides: A, T, C, and G (Figure 12c).

4. CONCLUSIONS AND OUTLOOK

Powerful single-molecule detection methods have provided a wealth of kinetic and thermodynamic molecular information of molecular activities toward establishing structure–functions relationship within life science fields. On a more practical note, single-molecule detection enables detailed and nondestructive analysis of precious samples on a time scale from nanoseconds to several minutes, providing a potential strategy for *in vivo* single-molecule imaging and ultrasensitive sensing. Beyond the technical challenges, single-molecule detection in life science investigations has the significant challenge of overcoming ensemble measurements that are more commonly used in biology. Integration of the present single-molecule real-time detection techniques will provide superior temporal-spatial resolution, allowing the precise investigation of biological dynamics. These methodologies established a fundamental for creating versatile, robust, universally available, low-cost, and precise toolbox for molecular or even future point-of-care clinical applications.

AUTHOR INFORMATION

Corresponding Author

*E-mail: guoxf@pku.edu.cn.

ORCID

Xuefeng Guo: 0000-0001-5723-8528

Author Contributions

†These authors contributed equally to this work.

Notes

The authors declare no competing financial interest.

ACKNOWLEDGMENTS

We acknowledge primary financial supports from National Key R&D Program of China (2017YFA0204901), the National Natural Science Foundation of China (21727806 and

21933001), the Natural Science Foundation of Beijing (Z181100004418003), and the interdisciplinary medicine Seed Fund of Peking University. X.G. acknowledges the support from the Tencent Foundation through the XPLOER PRIZE.

REFERENCES

- (1) Feynman, R. P. There's Plenty of Room at the Bottom. *Eng. Sci.* **1960**, *23* (5), 22–36.
- (2) Walter, N. G.; Huang, C.-Y.; Manzo, A. J.; Sobhy, M. A. Do-It-Yourself Guide: How to Use the Modern Single-Molecule Toolkit. *Nat. Methods* **2008**, *5* (6), 475–489.
- (3) Xiang, D.; Wang, X. L.; Jia, C. C.; Lee, T.; Guo, X. F. Molecular-Scale Electronics: From Concept to Function. *Chem. Rev.* **2016**, *116* (7), 4318–4440.
- (4) Xie, X. S.; Choi, P. J.; Li, G.-W.; Lee, N. K.; Lia, G. Single-Molecule Approach to Molecular Biology in Living Bacterial Cells. *Annu. Rev. Biophys.* **2008**, *37*, 417–444.
- (5) Roy, R.; Hohng, S.; Ha, T. A Practical Guide to Single-Molecule FRET. *Nat. Methods* **2008**, *5* (6), 507–516.
- (6) Jia, C. C.; Ma, B. J.; Xin, N.; Guo, X. F. Carbon Electrode-Molecule Junctions: A Reliable Platform for Molecular Electronics. *Acc. Chem. Res.* **2015**, *48* (9), 2565–2575.
- (7) Moerner, W. E.; Kador, L. Optical Detection and Spectroscopy of Single Molecules in a Solid. *Phys. Rev. Lett.* **1989**, *62* (21), 2535–2538.
- (8) Orrit, M.; Bernard, J. Single Pentacene Molecules Detected by Fluorescence Excitation in a *p*-Terphenyl Crystal. *Phys. Rev. Lett.* **1990**, *65* (21), 2716–2719.
- (9) Moerner, W. E. A Dozen Years of Single-Molecule Spectroscopy in Physics, Chemistry, and Biophysics. *J. Phys. Chem. B* **2002**, *106* (5), 910–927.
- (10) Dickson, R. M.; Norris, D. J.; Tzeng, Y.-L.; Moerner, W. Three-Dimensional Imaging of Single Molecules Solvated in Pores of Poly (Acrylamide) Gels. *Science* **1996**, *274* (5289), 966–968.
- (11) Funatsu, T.; Harada, Y.; Tokunaga, M.; Saito, K.; Yanagida, T. Imaging of Single Fluorescent Molecules and Individual ATP Turnovers by Single Myosin Molecules in Aqueous Solution. *Nature* **1995**, *374* (6522), 555–559.
- (12) Wasserman, M. R.; Alejo, J. L.; Altman, R. B.; Blanchard, S. C. Multiperspective smFRET Reveals Rate-Determining Late Intermediates of Ribosomal Translocation. *Nat. Struct. Mol. Biol.* **2016**, *23* (4), 333–341.
- (13) Lipman, E. A.; Schuler, B.; Bakajin, O.; Eaton, W. A. Single-Molecule Measurement of Protein Folding Kinetics. *Science* **2003**, *301* (5637), 1233–1235.
- (14) Chakraborty, A.; Wang, D.; Ebright, Y. W.; Korlann, Y.; Kortkhonjia, E.; Kim, T.; Chowdhury, S.; Wigneshweraraj, S.; Irschik, H.; Jansen, R.; et al. Opening and Closing of the Bacterial RNA Polymerase Clamp. *Science* **2012**, *337* (6094), 591–595.
- (15) Karunatilaka, K. S.; Solem, A.; Pyle, A. M.; Rueda, D. Single-Molecule Analysis of Mss116-Mediated Group II Intron Folding. *Nature* **2010**, *467* (7318), 935–939.
- (16) Mori, T.; Vale, R. D.; Tomishige, M. How Kinesin Waits Between Steps. *Nature* **2007**, *450* (7170), 750–754.
- (17) Chung, H. S.; McHale, K.; Louis, J. M.; Eaton, W. A. Single-Molecule Fluorescence Experiments Determine Protein Folding Transition Path Times. *Science* **2012**, *335* (6071), 981–984.
- (18) Zhuang, X.; Kim, H.; Pereira, M. J.; Babcock, H. P.; Walter, N. G.; Chu, S. Correlating Structural Dynamics and Function in Single Ribozyme Molecules. *Science* **2002**, *296* (5572), 1473–1476.
- (19) McKinney, S. A.; Déclais, A.-C.; Lilley, D. M. J.; Ha, T. Structural Dynamics of Individual Holliday Junctions. *Nat. Struct. Biol.* **2003**, *10* (2), 93–97.
- (20) Akyuz, N.; Altman, R. B.; Blanchard, S. C.; Boudker, O. Transport Dynamics in a Glutamate Transporter Homologue. *Nature* **2013**, *502* (7469), 114–118.

- (21) Kapanidis, A. N.; Strick, T. Biology, One Molecule at a Time. *Trends Biochem. Sci.* **2009**, *34* (5), 234–243.
- (22) Sharma, S.; Chakraborty, K.; Müller, B. K.; Astola, N.; Tang, Y.-C.; Lamb, D. C.; Hayer-Hartl, M.; Hartl, F. U. Monitoring Protein Conformation along the Pathway of Chaperonin-Assisted Folding. *Cell* **2008**, *133* (1), 142–153.
- (23) Maeder, C. I.; Hink, M. A.; Kinkhabwala, A.; Mayr, R.; Bastiaens, P. I. H.; Knop, M. Spatial Regulation of Fus3MAP Kinase Activity Through a Reaction-Diffusion Mechanism in Yeast Pheromone Signalling. *Nat. Cell Biol.* **2007**, *9* (11), 1319–1326.
- (24) Yu, S. R.; Burkhardt, M.; Nowak, M.; Ries, J.; Petrášek, Z.; Scholpp, S.; Schwill, P.; Brand, M. Fgf8 Morphogen Gradient Forms by a Source-Sink Mechanism with Freely Diffusing Molecules. *Nature* **2009**, *461* (7263), 533–536.
- (25) Du, Z. X.; Yu, J.; Li, F. C.; Deng, L. Y.; Wu, F.; Huang, X. Y.; Bergstrand, J.; Widengren, J.; Dong, C.; Ren, J. In Situ Monitoring of p53 Protein and MDM2 Protein Interaction in Single Living Cells Using Single-Molecule Fluorescence Spectroscopy. *Anal. Chem.* **2018**, *90* (10), 6144–6151.
- (26) Abbondanzieri, E. A.; Greenleaf, W. J.; Shaevitz, J. W.; Landick, R.; Block, S. M. Direct Observation of Base-Pair Stepping by RNA Polymerase. *Nature* **2005**, *438* (7067), 460–465.
- (27) Liphardt, J.; Onoa, B.; Smith, S. B.; Tinoco, I.; Bustamante, C. Reversible Unfolding of Single RNA Molecules by Mechanical Force. *Science* **2001**, *292* (5517), 733–737.
- (28) Koti Ainaravaru, S. R.; Wiita, A. P.; Dougan, L.; Uggerud, E.; Fernandez, J. M. Single-Molecule Force Spectroscopy Measurements of Bond Elongation during a Bimolecular Reaction. *J. Am. Chem. Soc.* **2008**, *130* (20), 6479–6487.
- (29) Hummer, G.; Szabo, A. Free Energy Surfaces from Single-Molecule Force Spectroscopy. *Acc. Chem. Res.* **2005**, *38* (7), 504–513.
- (30) Neuman, K. C.; Abbondanzieri, E. A.; Landick, R.; Gelles, J.; Block, S. M. Ubiquitous Transcriptional Pausing Is Independent of RNA Polymerase Backtracking. *Cell* **2003**, *115* (4), 437–447.
- (31) Li, W.; Hou, X.-M.; Wang, P.-Y.; Xi, X.-G.; Li, M. J. Direct Measurement of Sequential Folding Pathway and Energy Landscape of Human Telomeric G-quadruplex Structures. *J. Am. Chem. Soc.* **2013**, *135* (17), 6423–6426.
- (32) del Rio, A.; Perez-Jimenez, R.; Liu, R.; Roca-Cusachs, P.; Fernandez, J. M.; Sheetz, M. P. Stretching Single Talin Rod Molecules Activates Vinculin Binding. *Science* **2009**, *323* (5914), 638–641.
- (33) Manosas, M.; Perumal, S. K.; Croquette, V.; Benkovic, S. J. Direct Observation of Stalled Fork Restart via Fork Regression in the T4 Replication System. *Science* **2012**, *338* (6111), 1217–1220.
- (34) Kemmerich, F. E.; Swoboda, M.; Kauert, D. J.; Grieb, M. S.; Hahn, S.; Schwarz, F. W.; Seidel, R.; Schlierf, M. Simultaneous Single-Molecule Force and Fluorescence Sampling of DNA Nanostructure Conformations Using Magnetic Tweezers. *Nano Lett.* **2016**, *16* (1), 381–386.
- (35) Gore, J.; Bryant, Z.; Stone, M. D.; Nöllmann, M.; Cozzarelli, N. R.; Bustamante, C. Mechanochemical Analysis of DNA Gyrase Using Rotor Bead Tracking. *Nature* **2006**, *439* (7072), 100–104.
- (36) Collini, E.; Wong, C. Y.; Wilk, K. E.; Curmi, P. M. G.; Brumer, P.; Scholes, G. D. Coherently Wired Light-Harvesting in Photosynthetic Marine Algae at Ambient Temperature. *Nature* **2010**, *463* (7281), 644–647.
- (37) Brixner, T.; Stenger, J.; Vaswani, H. M.; Cho, M.; Blankenship, R. E.; Fleming, G. R. Two-Dimensional Spectroscopy of Electronic Couplings in Photosynthesis. *Nature* **2005**, *434* (7033), 625–628.
- (38) Engel, G. S.; Calhoun, T. R.; Read, E. L.; Ahn, T.-K.; Mančal, T.; Cheng, Y.-C.; Blankenship, R. E.; Fleming, G. R. Evidence for Wavelike Energy Transfer through Quantum Coherence in Photosynthetic Systems. *Nature* **2007**, *446* (7137), 782–786.
- (39) Panitchayangkoon, G.; Hayes, D.; Fransted, K. A.; Caram, J. R.; Harel, E.; Wen, J.; Blankenship, R. E.; Engel, G. S. Long-Lived Quantum Coherence in Photosynthetic Complexes at Physiological Temperature. *Proc. Natl. Acad. Sci. U. S. A.* **2010**, *107* (29), 12766–12770.
- (40) Baaske, M. D.; Foreman, M. R.; Vollmer, F. Single-Molecule Nucleic Acid Interactions Monitored on a Label-Free Microcavity Biosensor Platform. *Nat. Nanotechnol.* **2014**, *9* (11), 933–939.
- (41) Armani, A. M.; Kulkarni, R. P.; Fraser, S. E.; Flagan, R. C.; Vahala, K. J. Label-Free, Single-Molecule Detection with Optical Microcavities. *Science* **2007**, *317* (5839), 783–787.
- (42) Uchihashi, T.; Iino, R.; Ando, T.; Noji, H. High-Speed Atomic Force Microscopy Reveals Rotary Catalysis of Rotorless F1-ATPase. *Science* **2011**, *333* (6043), 755–758.
- (43) Oesterhelt, F.; Oesterhelt, D.; Pfeiffer, M.; Engel, A.; Gaub, H. E.; Müller, D. J. Unfolding Pathways of Individual Bacteriorhodopsins. *Science* **2000**, *288* (5463), 143–146.
- (44) Choi, Y.; Moody, I. S.; Sims, P. C.; Hunt, S. R.; Corso, B. L.; Perez, I.; Weiss, G. A.; Collins, P. G. Single-Molecule Lysozyme Dynamics Monitored by an Electronic Circuit. *Science* **2012**, *335* (6066), 319–324.
- (45) Olsen, T. J.; Choi, Y.; Sims, P. C.; Gul, O. T.; Corso, B. L.; Dong, C.; Brown, W. A.; Collins, P. G.; Weiss, G. A. Electronic Measurements of Single-Molecule Processing by DNA Polymerase I (Klenow Fragment). *J. Am. Chem. Soc.* **2013**, *135* (21), 7855–7860.
- (46) Sims, P. C.; Moody, I. S.; Choi, Y.; Dong, C.; Iftikhar, M.; Corso, B. L.; Gul, O. T.; Collins, P. G.; Weiss, G. A. Electronic Measurements of Single-Molecule Catalysis by cAMP-Dependent Protein Kinase A. *J. Am. Chem. Soc.* **2013**, *135* (21), 7861–7868.
- (47) Choi, Y.; Weiss, G. A.; Collins, P. G. Single Molecule Recordings of Lysozyme Activity. *Phys. Chem. Chem. Phys.* **2013**, *15* (36), 14879–14895.
- (48) Liu, S.; Zhang, X. Y.; Luo, W. X.; Wang, Z. X.; Guo, X. F.; Steigerwald, M. L.; Fang, X. Single-Molecule Detection of Proteins Using Aptamer-Functionalized Molecular Electronic Devices. *Angew. Chem., Int. Ed.* **2011**, *50* (11), 2496–2502.
- (49) Li, J.; He, G.; Ueno, H.; Jia, C. C.; Noji, H.; Qi, C. M.; Guo, X. F. Direct Real-Time Detection of Single Proteins Using Silicon Nanowire-Based Electrical Circuits. *Nanoscale* **2016**, *8* (36), 16172–16176.
- (50) Li, J.; He, G.; Hiroshi, U.; Liu, W. Z.; Noji, H.; Qi, C. M.; Guo, X. F. Direct Measurement of Single-Molecule Adenosine Triphosphatase Hydrolysis Dynamics. *ACS Nano* **2017**, *11* (12), 12789–12795.
- (51) He, G.; Li, J.; Ci, H. N.; Qi, C. M.; Guo, X. F. Direct Measurement of Single-Molecule DNA Hybridization Dynamics with Single-Base Resolution. *Angew. Chem.* **2016**, *128* (31), 9182–9186.
- (52) He, G.; Li, J.; Qi, C. M.; Guo, X. F. Single Nucleotide Polymorphism Genotyping in Single-Molecule Electronic Circuits. *Adv. Sci.* **2017**, *4* (11), 1700158.
- (53) Guo, X. F.; Gorodetsky, A. A.; Hone, J.; Barton, J. K.; Nuckolls, C. Conductivity of A Single DNA Duplex Bridging a Carbon Nanotube Gap. *Nat. Nanotechnol.* **2008**, *3* (3), 163–167.
- (54) Liu, S.; Clever, G. H.; Takezawa, Y.; Kaneko, M.; Tanaka, K.; Guo, X. F.; Shionoya, M. Direct Conductance Measurement of Individual Metallo-DNA Duplexes within Single-Molecule Break Junctions. *Angew. Chem.* **2011**, *123* (38), 9048–9052.
- (55) Venkatesan, B. M.; Bashir, R. Nanopore Sensors for Nucleic Acid Analysis. *Nat. Nanotechnol.* **2011**, *6* (10), 615–624.
- (56) Deamer, D.; Akeson, M.; Branton, D. Three Decades of Nanopore Sequencing. *Nat. Biotechnol.* **2016**, *34* (5), 518–524.
- (57) Liu, L.; Wu, H.-C. DNA-Based Nanopore Sensing. *Angew. Chem., Int. Ed.* **2016**, *55* (49), 15216–15222.
- (58) Valeur, B.; Berberan-Santos, M. N. A Brief History of Fluorescence and Phosphorescence before the Emergence of Quantum Theory. *J. Chem. Educ.* **2011**, *88* (6), 731–738.
- (59) Stokes, G. G. On the Change of Refrangibility of Light. *Philos. Trans. R. Soc. London* **1852**, *142*, 463–562.
- (60) Jablonski, A. Efficiency of Anti-Stokes Fluorescence in Dyes. *Nature* **1933**, *131* (3319), 839–840.
- (61) Ray, S.; Widom, J. R.; Walter, N. G. Life under the Microscope: Single-Molecule Fluorescence Highlights the RNA World. *Chem. Rev.* **2018**, *118* (8), 4120–4155.

- (62) Eigen, M.; Rigler, R. Sorting Single Molecules: Application to Diagnostics and Evolutionary Biotechnology. *Proc. Natl. Acad. Sci. U. S. A.* **1994**, *91* (13), 5740–5747.
- (63) Nakano, A. Spinning-disk Confocal Microscopy — A Cutting-Edge Tool for Imaging of Membrane Traffic. *Cell Struct. Funct.* **2002**, *27* (5), 349–355.
- (64) Axelrod, D.; Burghardt, T. P.; Thompson, N. L. Total Internal Reflection Fluorescence. *Annu. Rev. Biophys. Bioeng.* **1984**, *13* (1), 247–268.
- (65) Huisken, J.; Swoger, J.; Del Bene, F.; Wittbrodt, J.; Stelzer, E. H. K. Optical Sectioning Deep Inside Live Embryos by Selective Plane Illumination Microscopy. *Science* **2004**, *305* (5686), 1007–1009.
- (66) Denk, W.; Strickler, J.; Webb, W. Two-Photon Laser Scanning Fluorescence Microscopy. *Science* **1990**, *248* (4951), 73–76.
- (67) Betzig, E.; Chichester, R. J. Single Molecules Observed by Near-Field Scanning Optical Microscopy. *Science* **1993**, *262* (5138), 1422–1425.
- (68) Yildiz, A.; Selvin, P. R. Fluorescence Imaging with One Nanometer Accuracy: Application to Molecular Motors. *Acc. Chem. Res.* **2005**, *38* (7), 574–582.
- (69) Rosenberg, S. A.; Quinlan, M. E.; Forkey, J. N.; Goldman, Y. E. Rotational Motions of Macro-molecules by Single-Molecule Fluorescence Microscopy. *Acc. Chem. Res.* **2005**, *38* (7), 583–593.
- (70) Lu, H. P.; Xun, L.; Xie, X. S. Single-Molecule Enzymatic Dynamics. *Science* **1998**, *282* (5395), 1877–1882.
- (71) Benoit, M. P. M. H.; Sosa, H. Use of Single Molecule Fluorescence Polarization Microscopy to Study Protein Conformation and Dynamics of Kinesin-Microtubule Complexes. In *Single Molecule Analysis: Methods and Protocols*; Peterman, E. J. G., Ed.; Springer: New York, 2018; pp 199–216.
- (72) Duzdevich, D.; Redding, S.; Greene, E. C. DNA Dynamics and Single-Molecule Biology. *Chem. Rev.* **2014**, *114* (6), 3072–3086.
- (73) van Oijen, A. M. Single-Molecule Approaches to Characterizing Kinetics of Biomolecular Interactions. *Curr. Opin. Biotechnol.* **2011**, *22* (1), 75–80.
- (74) Cario, G.; Franck, J. Nuclei, Über Sensibilisierte Fluoreszenz Von Gasen. *Eur. Phys. J. A* **1923**, *17* (1), 202–212.
- (75) Stryer, L. Fluorescence Energy Transfer as a Spectroscopic Ruler. *Annu. Rev. Biochem.* **1978**, *47* (1), 819–846.
- (76) Lerner, E.; Cordes, T.; Ingarciola, A.; Alhadid, Y.; Chung, S.; Michalet, X.; Weiss, S. J. S. Toward Dynamic Structural Biology: Two Decades of Single-Molecule Förster Resonance Energy Transfer. *Science* **2018**, *359* (6373), No. eaan1133.
- (77) Ha, T.; Enderle, T.; Ogletree, D.; Chemla, D. S.; Selvin, P. R.; Weiss, S. Probing the Interaction Between Two Single Molecules: Fluorescence Resonance Energy Transfer Between a Single Donor and a Single Acceptor. *Proc. Natl. Acad. Sci. U. S. A.* **1996**, *93* (13), 6264–6268.
- (78) Deniz, A. A.; Dahan, M.; Grunwell, J. R.; Ha, T.; Faulhaber, A. E.; Chemla, D. S.; Weiss, S.; Schultz, P. G. Single-Pair Fluorescence Resonance Energy Transfer on Freely Diffusing Molecules: Observation of Förster Distance Dependence and Subpopulations. *Proc. Natl. Acad. Sci. U. S. A.* **1999**, *96* (7), 3670–3675.
- (79) Schuler, B.; Lipman, E. A.; Eaton, W. A. Probing the Free-Energy Surface for Protein Folding with Single-Molecule Fluorescence Spectroscopy. *Nature* **2002**, *419* (6908), 743–747.
- (80) Kapanidis, A. N.; Lee, N. K.; Laurence, T. A.; Doose, S.; Margeat, E.; Weiss, S. Fluorescence-Aided Molecule Sorting: Analysis of Structure and Interactions by Alternating-Laser Excitation of Single Molecules. *Proc. Natl. Acad. Sci. U. S. A.* **2004**, *101* (24), 8936–8941.
- (81) Kapanidis, A. N.; Margeat, E.; Ho, S. O.; Kortkhonjia, E.; Weiss, S.; Ebright, R. H. Initial Transcription by RNA Polymerase Proceeds Through a DNA-Scrunching Mechanism. *Science* **2006**, *314* (5802), 1144–1147.
- (82) Diez, M.; Zimmermann, B.; Börsch, M.; König, M.; Schweinberger, E.; Steigmiller, S.; Reuter, R.; Felekyan, S.; Kudryavtsev, V.; Seidel, C. A.; et al. Proton-Powered Subunit Rotation in Single Membrane-Bound F₀F₁-ATP Synthase. *Nat. Struct. Mol. Biol.* **2004**, *11* (2), 135–141.
- (83) Rüttinger, S.; Macdonald, R.; Krämer, B.; Koberling, F.; Roos, M.; Hildt, E. Accurate Single-Pair Förster Resonant Energy Transfer through Combination of Pulsed Interleaved Excitation, Time Correlated Single-Photon Counting, and Fluorescence Correlation Spectroscopy. *J. Biomed. Opt.* **2006**, *11* (2), 024012.
- (84) Ferreon, A. C. M.; Ferreon, J. C.; Wright, P. E.; Deniz, A. A. Modulation of Allostery by Protein Intrinsic Disorder. *Nature* **2013**, *498* (7454), 390–394.
- (85) Zhuang, X. W.; Bartley, L. E.; Babcock, H. P.; Russell, R.; Ha, T.; Herschlag, D.; Chu, S. A Single-Molecule Study of RNA Catalysis and Folding. *Science* **2000**, *288* (5473), 2048–2051.
- (86) Tan, E.; Wilson, T. J.; Nahas, M. K.; Clegg, R. M.; Lilley, D. M.; Ha, T. A Four-Way Junction Accelerates Hairpin Ribozyme Folding via a Discrete Intermediate. *Proc. Natl. Acad. Sci. U. S. A.* **2003**, *100* (16), 9308–9313.
- (87) Liu, S. X.; Bokinsky, G.; Walter, N. G.; Zhuang, X. W. Dissecting the Multistep Reaction Pathway of an RNA Enzyme by Single-Molecule Kinetic “Fingerprinting”. *Proc. Natl. Acad. Sci. U. S. A.* **2007**, *104* (31), 12634–12639.
- (88) Ha, T.; Rasnik, I.; Cheng, W.; Babcock, H. P.; Gauss, G. H.; Lohman, T. M.; Chu, S. Initiation and Re-Initiation of DNA Unwinding by the *Escherichia Coli* Rep Helicase. *Nature* **2002**, *419* (6907), 638–641.
- (89) Joo, C.; McKinney, S. A.; Nakamura, M.; Rasnik, I.; Myong, S.; Ha, T. Real-Time Observation of RecA Filament Dynamics with Single Monomer Resolution. *Cell* **2006**, *126* (3), 515–527.
- (90) Stone, M. D.; Mihalusova, M.; O’Connor, C. M.; Prathapam, R.; Collins, K.; Zhuang, X. Stepwise Protein-Mediated RNA Folding Directs Assembly of Telomerase Ribonucleoprotein. *Nature* **2007**, *446* (7134), 458–461.
- (91) Groll, J.; Amirgoulova, E. V.; Ameringer, T.; Heyes, C. D.; Röcker, C.; Nienhaus, G. U.; Möller, M. Biofunctionalized, Ultrathin Coatings of Cross-Linked Star-Shaped Poly (Ethylene Oxide) Allow Reversible Folding of Immobilized Proteins. *J. Am. Chem. Soc.* **2004**, *126* (13), 4234–4239.
- (92) Eid, J.; Fehr, A.; Gray, J.; Luong, K.; Lyle, J.; Otto, G.; Peluso, P.; Rank, D.; Baybayan, P.; Bettman, B.; et al. Real-Time DNA Sequencing from Single Polymerase Molecules. *Science* **2009**, *323* (5910), 133–138.
- (93) Levene, M. J.; Korlach, J.; Turner, S. W.; Foquet, M.; Craighead, H. G.; Webb, W. W. Zero-Mode Waveguides for Single-Molecule Analysis at High Concentrations. *Science* **2003**, *299* (5607), 682–686.
- (94) Rhoades, E.; Gussakovskiy, E.; Haran, G. Watching Proteins Fold One Molecule at A Time. *Proc. Natl. Acad. Sci. U. S. A.* **2003**, *100* (6), 3197–3202.
- (95) Cisse, I.; Okumus, B.; Joo, C.; Ha, T. Fueling Protein-DNA Interactions Inside Porous Nanocontainers. *Proc. Natl. Acad. Sci. U. S. A.* **2007**, *104* (31), 12646–12650.
- (96) Elson, E. L. Fluorescence Correlation Spectroscopy: Past, Present, Future. *Biophys. J.* **2011**, *101* (12), 2855–2870.
- (97) Tian, Y.; Martinez, M. M.; Pappas, D. Fluorescence Correlation Spectroscopy: A Review of Biochemical and Microfluidic Applications. *Appl. Spectrosc.* **2011**, *65* (4), 115A–124A.
- (98) Leutenegger, M.; Ringemann, C.; Lasser, T.; Hell, S. W.; Eggeling, C. Fluorescence Correlation Spectroscopy with A Total Internal Reflection Fluorescence STED Microscope (TIRF-STED-FCS). *Opt. Express* **2012**, *20* (5), 5243–5263.
- (99) Wohland, T.; Shi, X. K.; Sankaran, J.; Stelzer, E. H. K. Single Plane Illumination Fluorescence Correlation Spectroscopy (SPIM-FCS) Probes Inhomogeneous Three-Dimensional Environments. *Opt. Express* **2010**, *18* (10), 10627–10641.
- (100) Krieger, J. W.; Singh, A. P.; Bag, N.; Garbe, C. S.; Saunders, T. E.; Langowski, J.; Wohland, T. Imaging Fluorescence (Cross-) Correlation Spectroscopy in Live Cells and Organisms. *Nat. Protoc.* **2015**, *10*, 1948–1974.

- (101) Ries, J.; Schwille, P. Fluorescence Correlation Spectroscopy. *BioEssays* **2012**, *34* (5), 361–368.
- (102) Hess, S. T.; Huang, S. H.; Heikal, A. A.; Webb, W. W. Biological and Chemical Applications of Fluorescence Correlation Spectroscopy: A Review. *Biochemistry* **2002**, *41* (3), 697–705.
- (103) Hausteiner, E.; Schwille, P. Single-Molecule Spectroscopic Methods. *Curr. Opin. Struct. Biol.* **2004**, *14* (5), 531–540.
- (104) Altan-Bonnet, G.; Libchaber, A.; Krichevsky, O. Bubble Dynamics in Double-Stranded DNA. *Phys. Rev. Lett.* **2003**, *90* (13), 138101.
- (105) Chen, X. D.; Zhou, Y.; Qu, P.; Zhao, X. S. Base-by-Base Dynamics in DNA Hybridization Probed by Fluorescence Correlation Spectroscopy. *J. Am. Chem. Soc.* **2008**, *130* (50), 16947–16952.
- (106) Hausteiner, E.; Schwille, P. Ultrasensitive Investigations of Biological Systems by Fluorescence Correlation Spectroscopy. *Methods* **2003**, *29* (2), 153–166.
- (107) Simpson, L. W.; Szeto, G. L.; Boukari, H.; Good, T. A.; Leach, J. B. Impact of Four Common Hydrogels on Amyloid- β (A β) Aggregation and Cytotoxicity: Implications for 3D Models of Alzheimer's Disease. *BioRxiv* **2019**, 711770 DOI: 10.1101/711770.
- (108) Tamura, T.; Endo, H.; Suzuki, A.; Sato, Y.; Kato, K.; Ohtani, M.; Yamaguchi, M.; Demura, T. Affinity-Based High-Resolution Analysis of DNA Binding by VASCULAR-RELATED NAC-DOMAIN7 via Fluorescence Correlation Spectroscopy. *Plant J.* **2019**, *100*, 298–313.
- (109) Cao, C. Y.; Jiang, Y. L.; Stivers, J. T.; Song, F. H. Dynamic Opening of DNA During the Enzymatic Search for a Damaged Base. *Nat. Struct. Mol. Biol.* **2004**, *11* (12), 1230–1236.
- (110) Yang, C. G.; Garcia, K.; He, C. Damage Detection and Base Flipping in Direct DNA Alkylation Repair. *ChemBioChem* **2009**, *10* (3), 417–423.
- (111) Parker, J. B.; Bianchet, M. A.; Krosky, D. J.; Friedman, J. I.; Amzel, L. M.; Stivers, J. T. Enzymatic Capture of an Extrahelical Thymine in the Search for Uracil in DNA. *Nature* **2007**, *449* (7161), 433–437.
- (112) Chen, Y. Z.; Mohan, V.; Griffey, R. Spontaneous Base Flipping in DNA and Its Possible Role in Methyltransferase Binding. *Phys. Rev. E: Stat. Phys., Plasmas, Fluids, Relat. Interdiscip. Top.* **2000**, *62* (1), 1133–1137.
- (113) Yin, Y. D.; Yang, L. J.; Zheng, G. Q.; Gu, C.; Yi, C. Q.; He, C.; Gao, Y. Q.; Zhao, X. S. Dynamics of Spontaneous Flipping of A Mismatched Base in DNA Duplex. *Proc. Natl. Acad. Sci. U. S. A.* **2014**, *111* (22), 8043–8048.
- (114) Magde, D.; Elson, E.; Webb, W. W. Thermodynamic Fluctuations in a Reacting System-Measurement by Fluorescence Correlation Spectroscopy. *Phys. Rev. Lett.* **1972**, *29* (11), 705–708.
- (115) Edman, L.; Mets, U.; Rigler, R. Conformational Transitions Monitored for Single Molecules in Solution. *Proc. Natl. Acad. Sci. U. S. A.* **1996**, *93* (13), 6710–6715.
- (116) Yin, Y. D.; Wang, P.; Yang, X. X.; Li, X.; He, C.; Zhao, X. S. Panorama of DNA Hairpin Folding Observed via Diffusion-Decelerated Fluorescence Correlation Spectroscopy. *Chem. Commun.* **2012**, *48* (59), 7413–7415.
- (117) Dallmann, A.; Dehmel, L.; Peters, T.; Mügge, C.; Griesinger, C.; Tuma, J.; Ernsting, N. P. 2-Aminopurine Incorporation Perturbs the Dynamics and Structure of DNA. *Angew. Chem. Int. Ed.* **2010**, *49* (34), 5989–5992.
- (118) Klimašauskas, S.; Szyperski, T.; Serva, S.; Wüthrich, K. Dynamic Modes of The Flipped-Out Cytosine During HhaI Methyltransferase-DNA Interactions in Solution. *EMBO J.* **1998**, *17* (1), 317–324.
- (119) Moe, J. G.; Russu, I. M. Kinetics and Energetics of Base-Pair Opening in 5'-d (CGCGAATTCGCG)-3' and a Substituted Dodecamer Containing G. Cntdot. T Mismatches. *Biochemistry* **1992**, *31* (36), 8421–8428.
- (120) Schwille, P.; Meyer-Almes, F. J.; Rigler, R. Dual-Color Fluorescence Cross-Correlation Spectroscopy for Multicomponent Diffusional Analysis in Solution. *Biophys. J.* **1997**, *72* (4), 1878–1886.
- (121) Kettling, U.; Koltermann, A.; Schwille, P.; Eigen, M. Real-Time Enzyme Kinetics Monitored by Dual-Color Fluorescence Cross-Correlation Spectroscopy. *Proc. Natl. Acad. Sci. U. S. A.* **1998**, *95* (4), 1416–1420.
- (122) Slavik, J. *Fluorescence microscopy and fluorescent probes*. Plenum Press: New York, 1996.
- (123) Bacia, K.; Majoul, I. V.; Schwille, P. Probing the Endocytic Pathway in Live Cells Using Dual-Color Fluorescence Cross-Correlation Analysis. *Biophys. J.* **2002**, *83* (2), 1184–1193.
- (124) Moffitt, J. R.; Chemla, Y. R.; Smith, S. B.; Bustamante, C. Recent Advances in Optical Tweezers. *Annu. Rev. Biochem.* **2008**, *77*, 205–228.
- (125) Ashkin, A.; Dziedzic, J. M.; Bjorkholm, J. E.; Chu, S. Observation of a Single-Beam Gradient Force Optical Trap for Dielectric Particles. *Opt. Lett.* **1986**, *11* (5), 288–290.
- (126) Clausen-Schaumann, H.; Seitz, M.; Krautbauer, R.; Gaub, H. E. Force Spectroscopy with Single Bio-Molecules. *Curr. Opin. Chem. Biol.* **2000**, *4* (5), 524–530.
- (127) Block, S. M.; Goldstein, L. S. B.; Schnapp, B. J. Bead Movement by Single Kinesin Molecules Studied with Optical Tweezers. *Nature* **1990**, *348* (6299), 348–352.
- (128) Yu, H.; Gupta, A. N.; Liu, X.; Neupane, K.; Brigley, A. M.; Sosova, I.; Woodside, M. T. Energy Landscape Analysis of Native Folding of the Prion Protein Yields the Diffusion Constant, Transition Path Time, and Rates. *Proc. Natl. Acad. Sci. U. S. A.* **2012**, *109* (36), 14452–14457.
- (129) Cecconi, C.; Shank, E. A.; Bustamante, C.; Marqusee, S. Direct Observation of the Three-State Folding of a Single Protein Molecule. *Science* **2005**, *309* (5743), 2057–2060.
- (130) Neuman, K. C.; Nagy, A. Single-Molecule Force Spectroscopy: Optical Tweezers, Magnetic Tweezers and Atomic Force Microscopy. *Nat. Methods* **2008**, *5*, 491–505.
- (131) Shrestha, P.; Jonchhe, S.; Emura, T.; Hidaka, K.; Endo, M.; Sugiyama, H.; Mao, H. Confined Space Facilitates G-quadruplex Formation. *Nat. Nanotechnol.* **2017**, *12* (6), 582–588.
- (132) Strick, T. R.; Croquette, V.; Bensimon, D. J. N. Single-Molecule Analysis of DNA Uncoiling by a Type II Topoisomerase. *Nature* **2000**, *404* (6780), 901–904.
- (133) Maiman, T. H. Stimulated Optical Radiation in Ruby. *Nature* **1960**, *187*, 493–494.
- (134) Dean, J. C.; Mirkovic, T.; Toa, Z. S. D.; Oblinsky, D. G.; Scholes, G. D. Vibronic Enhancement of Algae Light Harvesting. *Chem.* **2016**, *1* (6), 858–872.
- (135) Blau, S. M.; Bennett, D. I. G.; Kreisbeck, C.; Scholes, G. D.; Aspuru-Guzik, A. Local Protein Solvation Drives Direct Down-Conversion in Phycobiliprotein PC645 via Incoherent Vibronic Transport. *Proc. Natl. Acad. Sci. U. S. A.* **2018**, *115* (15), E3342–E3350.
- (136) Schlau-Cohen, G. S.; Ishizaki, A.; Calhoun, T. R.; Ginsberg, N. S.; Ballottari, M.; Bassi, R.; Fleming, G. R. Elucidation of the Timescales and Origins of Quantum Electronic Coherence in LHClI. *Nat. Chem.* **2012**, *4* (5), 389–395.
- (137) Paleček, D.; Edlund, P.; Westenhoff, S.; Zigmantas, D. Quantum Coherence as A Witness of Vibronically Hot Energy Transfer in Bacterial Reaction Center. *Sci. Adv.* **2017**, *3* (9), No. e1603141.
- (138) Romero, E.; Augulis, R.; Novoderezhkin, V. I.; Ferretti, M.; Thieme, J.; Zigmantas, D.; van Grondelle, R. Quantum Coherence in Photosynthesis for Efficient Solar-Energy Conversion. *Nat. Phys.* **2014**, *10* (9), 676–682.
- (139) Washburn, A. L.; Gunn, L. C.; Bailey, R. C. Label-Free Quantitation of a Cancer Biomarker in Complex Media Using Silicon Photonic Microring Resonators. *Anal. Chem.* **2009**, *81* (22), 9499–9506.
- (140) Vollmer, F.; Yang, L. Review Label-Free Detection with High-Q Microcavities: A Review of Biosensing Mechanisms for Integrated Devices. *Nanophotonics* **2012**, *1* (3–4), 267–291.

- (141) Robinson, J. T.; Chen, L.; Lipson, M. On-Chip Gas Detection in Silicon Optical Microcavities. *Opt. Express* **2008**, *16* (6), 4296–4301.
- (142) Lu, T.; Lee, H.; Chen, T.; Herchak, S.; Kim, J.-H.; Fraser, S. E.; Flagan, R. C.; Vahala, K. High Sensitivity Nanoparticle Detection Using Optical Microcavities. *Proc. Natl. Acad. Sci. U. S. A.* **2011**, *108* (15), 5976–5979.
- (143) Vollmer, F.; Arnold, S. Whispering-Gallery-Mode Biosensing: Label-Free Detection Down to Single Molecules. *Nat. Methods* **2008**, *5* (7), 591–596.
- (144) Vollmer, F.; Arnold, S.; Keng, D. Single Virus Detection from the Reactive Shift of a Whispering-Gallery Mode. *Proc. Natl. Acad. Sci. U. S. A.* **2008**, *105* (52), 20701–20704.
- (145) Binnig, G.; Gerber, C.; Stoll, E.; Albrecht, T.; Quate, C. Atomic Resolution with Atomic Force Microscope. *EPL (Europhys. Lett.)* **1987**, *3* (12), 1281–1286.
- (146) Rajendran, A.; Endo, M.; Sugiyama, H. State-of-the-Art High-Speed Atomic Force Microscopy for Investigation of Single-Molecular Dynamics of Proteins. *Chem. Rev.* **2014**, *114* (2), 1493–1520.
- (147) Zhong, Q.; Inniss, D.; Kjoller, K.; Elings, V. Fractured Polymer/Silica Fiber Surface Studied by Tapping Mode Atomic Force Microscopy. *Surf. Sci.* **1993**, *290* (1–2), L688–L692.
- (148) Marti, O.; Drake, B.; Hansma, P. K. Atomic Force Microscopy of Liquid-Covered Surfaces: Atomic Resolution Images. *Appl. Phys. Lett.* **1987**, *51* (7), 484–486.
- (149) Kodera, N.; Yamamoto, D.; Ishikawa, R.; Ando, T. Video Imaging of Walking Myosin V by High-Speed Atomic Force Microscopy. *Nature* **2010**, *468* (7320), 72–76.
- (150) Ando, T.; Kodera, N.; Uchihashi, T.; Miyagi, A.; Nakakita, R.; Yamashita, H.; Matada, K. High-speed Atomic Force Microscopy for Capturing Dynamic Behavior of Protein Molecules at Work. *e-J. Surf. Sci. Nanotechnol.* **2005**, *3*, 384–392.
- (151) Yokokawa, M.; Yoshimura, S. H.; Naito, Y.; Ando, T.; Yagi, A.; Sakai, N.; Takeyasu, K. Fast-Scanning Atomic Force Microscopy Reveals the Molecular Mechanism of DNA Cleavage by Apal Endonuclease. *IEE Proc.: Nanobiotechnol.* **2006**, *153* (4), 60–66.
- (152) Iijima, S. Helical Microtubules of Graphitic Carbon. *Nature* **1991**, *354* (6348), 56–58.
- (153) Schnorr, J. M.; Swager, T. M. Emerging Applications of Carbon Nanotubes. *Chem. Mater.* **2011**, *23* (3), 646–657.
- (154) Münzer, A. M.; Michael, Z. P.; Star, A. Carbon Nanotubes for the Label-Free Detection of Biomarkers. *ACS Nano* **2013**, *7* (9), 7448–7453.
- (155) Lu, F.; Gu, L.; Mezzani, M. J.; Wang, X.; Luo, P. G.; Veca, L. M.; Cao, L.; Sun, Y. P. Advances in Bioapplications of Carbon Nanotubes. *Adv. Mater.* **2009**, *21* (2), 139–152.
- (156) Balasubramanian, K.; Kern, K. 25th Anniversary Article: Label-Free Electrical Biodetection Using Carbon Nanostructures. *Adv. Mater.* **2014**, *26* (8), 1154–1175.
- (157) Choi, Y.; Olsen, T. J.; Sims, P. C.; Moody, I. S.; Corso, B. L.; Dang, M. N.; Weiss, G. A.; Collins, P. G. Dissecting Single-Molecule Signal Transduction in Carbon Nanotube Circuits with Protein Engineering. *Nano Lett.* **2013**, *13* (2), 625–631.
- (158) Goldsmith, B. R.; Coroneus, J. G.; Khalap, V. R.; Kane, A. A.; Weiss, G. A.; Collins, P. G. Conductance-Controlled Point Functionalization of Single-Walled Carbon Nanotubes. *Science* **2007**, *315* (5808), 77–81.
- (159) Goldsmith, B. R.; Coroneus, J. G.; Kane, A. A.; Weiss, G. A.; Collins, P. G. Monitoring Single-Molecule Reactivity on a Carbon Nanotube. *Nano Lett.* **2008**, *8* (1), 189–194.
- (160) Sorgenfrei, S.; Chiu, C.-y.; Gonzalez, R. L., Jr; Yu, Y.-J.; Kim, P.; Nuckolls, C.; Shepard, K. L. Label-Free Single-Molecule Detection of DNA-Hybridization Kinetics with A Carbon Nanotube Field-Effect Transistor. *Nat. Nanotechnol.* **2011**, *6* (2), 126–132.
- (161) Sorgenfrei, S.; Chiu, C.-y.; Johnston, M.; Nuckolls, C.; Shepard, K. L. Debye Screening in Single-Molecule Carbon Nanotube Field-Effect Sensors. *Nano Lett.* **2011**, *11* (9), 3739–3743.
- (162) Guo, X.; Myers, M.; Xiao, S.; Lefenfeld, M.; Steiner, R.; Tulevski, G. S.; Tang, J.; Baumert, J.; Leibfarth, F.; Yardley, J. T.; et al. Chemoresponsive Monolayer Transistors. *Proc. Natl. Acad. Sci. U. S. A.* **2006**, *103* (31), 11452–11456.
- (163) Jia, C. C.; Migliore, A.; Xin, N.; Huang, S. Y.; Wang, J. Y.; Yang, Q.; Wang, S. P.; Chen, H. L.; Wang, D. M.; Feng, B. Y.; Liu, Z. R.; Zhang, G. Y.; Qu, D. H.; Tian, H.; Ratner, M. A.; Xu, H. Q.; Nitzan, A.; Guo, X. F. Covalently Bonded Single-Molecule Junctions with Stable and Reversible Photoswitched Conductivity. *Science* **2016**, *352* (6292), 1443–1445.
- (164) Whalley, A. C.; Steigerwald, M. L.; Guo, X. F.; Nuckolls, C. Reversible Switching in Molecular Electronic Devices. *J. Am. Chem. Soc.* **2007**, *129* (42), 12590–12591.
- (165) Genereux, J. C.; Barton, J. K. Mechanisms for DNA Charge Transport. *Chem. Rev.* **2010**, *110* (3), 1642–1662.
- (166) Guo, X.; Small, J. P.; Klare, J. E.; Wang, Y.; Purewal, M. S.; Tam, I. W.; Hong, B. H.; Caldwell, R.; Huang, L.; O'Brien, S.; et al. Covalently Bridging Gaps in Single-Walled Carbon Nanotubes with Conducting Molecules. *Science* **2006**, *311* (5759), 356–359.
- (167) Patolsky, F.; Zheng, G.; Hayden, O.; Lakadamyali, M.; Zhuang, X.; Lieber, C. M. Electrical Detection of Single Viruses. *Proc. Natl. Acad. Sci. U. S. A.* **2004**, *101* (39), 14017–14022.
- (168) Shen, F. X.; Wang, J. D.; Xu, Z. Q.; Wu, Y.; Chen, Q.; Li, X. G.; Jie, X.; Li, L. D.; Yao, M. S.; Guo, X. F.; et al. Rapid Flu Diagnosis Using Silicon Nanowire Sensor. *Nano Lett.* **2012**, *12* (7), 3722–3730.
- (169) Wang, J. D.; Shen, F. X.; Wang, Z. X.; He, G.; Qin, J. W.; Cheng, N. Y.; Yao, M. S.; Li, L. D.; Guo, X. F. Point Decoration of Silicon Nanowires: An Approach Toward Single-Molecule Electrical Detection. *Angew. Chem.* **2014**, *126* (20), 5138–5143.
- (170) Feng, J. D.; Liu, K.; Bulushev, R. D.; Khlybov, S.; Dumcenco, D.; Kis, A.; Radenovic, A. Identification of Single Nucleotides in MoS₂ Nanopores. *Nat. Nanotechnol.* **2015**, *10* (12), 1070–1076.
- (171) Akeson, M.; Branton, D.; Kasianowicz, J. J.; Brandin, E.; Deamer, D. W. Microsecond Time-Scale Discrimination among Polycytidylic Acid, Polyadenylic Acid, and Polyuridylic Acid as Homopolymers Or as Segments within Single RNA Molecules. *Biophys. J.* **1999**, *77* (6), 3227–3233.
- (172) Meller, A.; Branton, D. Single Molecule Measurements of DNA Transport Through a Nanopore. *Electrophoresis* **2002**, *23* (16), 2583–2591.
- (173) Ashkenasy, N.; Sánchez-Quesada, J.; Bayley, H.; Ghadiri, M. R. Recognizing A Single Base in an Individual DNA Strand: An Step Toward DNA Sequencing in Nanopores. *Angew. Chem.* **2005**, *117* (9), 1425–1428.
- (174) Stoddart, D.; Heron, A. J.; Mikhailova, E.; Maglia, G.; Bayley, H. Single-Nucleotide Discrimination in Immobilized DNA Oligonucleotides with a Biological Nanopore. *Proc. Natl. Acad. Sci. U. S. A.* **2009**, *106* (19), 7702–7707.
- (175) Cherf, G. M.; Lieberman, K. R.; Rashid, H.; Lam, C. E.; Karplus, K.; Akeson, M. Automated Forward and Reverse Ratcheting of DNA in a Nanopore at 5-Å Precision. *Nat. Biotechnol.* **2012**, *30* (4), 344–348.
- (176) Manrao, E. A.; Derrington, I. M.; Laszlo, A. H.; Langford, K. W.; Hopper, M. K.; Gillgren, N.; Pavlenok, M.; Niederweis, M.; Gundlach, J. H. Reading DNA at Single-Nucleotide Resolution with A Mutant MspA Nanopore and phi29 DNA Polymerase. *Nat. Biotechnol.* **2012**, *30* (4), 349–353.
- (177) Wang, Y.; Patil, K. M.; Yan, S. H.; Zhang, P. K.; Guo, W. M.; Wang, Y. Q.; Chen, H.-Y.; Gillingham, D.; Huang, S. Nanopore Sequencing Accurately Identifies the Mutagenic DNA Lesion O₆-Carboxymethyl Guanine and Reveals Its Behavior in Replication. *Angew. Chem., Int. Ed.* **2019**, *58* (25), 8432–8436.
- (178) Laszlo, A. H.; Derrington, I. M.; Ross, B. C.; Brinkerhoff, H.; Aday, A.; Nova, I. C.; Craig, J. M.; Langford, K. W.; Samson, J. M.; Daza, R.; Doering, K.; Shendure, J.; Gundlach, J. H. Decoding Long Nanopore Sequencing Reads of Natural DNA. *Nat. Biotechnol.* **2014**, *32* (8), 829–833.
- (179) Storm, A. J.; Chen, J. H.; Ling, X. S.; Zandbergen, H.; Dekker, C. Fabrication of Solid-State Nanopores with Single-Nanometre Precision. *Nat. Mater.* **2003**, *2* (8), 537–540.

(180) Venkatesan, B. M.; Dorvel, B.; Yemenicioglu, S.; Watkins, N.; Petrov, I.; Bashir, R. Highly Sensitive, Mechanically Stable Nanopore Sensors for DNA Analysis. *Adv. Mater.* **2009**, *21* (27), 2771–2776.

(181) Li, J. L.; Stein, D.; McMullan, C.; Branton, D.; Aziz, M. J.; Golovchenko, J. A. Ion-Beam Sculpting at Nanometre Length Scales. *Nature* **2001**, *412* (6843), 166–169.

(182) Garaj, S.; Hubbard, W.; Reina, A.; Kong, J.; Branton, D.; Golovchenko, J. Graphene as A Subnanometre Trans-Electrode Membrane. *Nature* **2010**, *467* (7312), 190–193.

(183) Schneider, G. F.; Kowalczyk, S. W.; Calado, V. E.; Pandraud, G.; Zandbergen, H. W.; Vandersypen, L. M.; Dekker, C. DNA Translocation through Graphene Nanopores. *Nano Lett.* **2010**, *10* (8), 3163–3167.

(184) Merchant, C. A.; Healy, K.; Wanunu, M.; Ray, V.; Peterman, N.; Bartel, J.; Fischbein, M. D.; Venta, K.; Luo, Z.; Johnson, A. C.; et al. DNA Translocation through Graphene Nanopores. *Nano Lett.* **2010**, *10* (8), 2915–2921.